UNIVERSITY OF MALAYA

# Thermoelectric Materials and Devices for Power Generation

**Ir Dr Mohd Faizul Mohd Sabri**
Associate Professor
Deputy Dean (Research)

faizul@um.edu.my

Faculty of Engineering
University of Malaya, Malaysia

# Outline

- Introduction to University of Malaya
- Thermoelectric
  - Introduction and fundamental principle
  - Current state of development and applications
  - Works at the lab of NanoMicro Engineering

# University of Malaya

- Established in 1949

# Campus View

# History

The **King Edward VII College of Medicine** was founded in **1905** to train the first Malaysian (Malayan) doctors. The College later became known as the University of Malaya in Singapore.

The University of Malaya **Kuala Lumpur campus** was established in **1959**.

The **University Hospital** was opened in **1968**.

**Present** day University of Malaya.

**1905**

King Edward VII College of Medicine, Singapore

**1928**

Raffles College Singapore

**1949**

Raffles College was merged with King Edward VII College of Medicine to become the University of Malaya.

**1962**

University of Singapore (now known as National University of Singapore)

University of Malaya Kuala Lumpur

# UM Profile

**12** Faculties

**2** Academies

**3** Centers

**3** Institutes

**4** Research Clusters

**>50** Research Centres

**1** Private University

**1** Continuing Education Centre

**>17,000** Undergraduate Students

**>13,000** Postgraduate Students

**>30,000** Total Number of Students

**>3,700** International Students from over **90** Countries

Over **200** Academic Programmes

**>6,000**
Total Staff Strength

**>2,300**
Academic Staff
13.5% International

**>2,900**
Support Staff

**>670**
Management & Professional

**INTERNATIONAL ACADEMIC STAFF FROM MORE THAN 60 COUNTRIES INCLUDES:**

| | | | |
|---|---|---|---|
| Algeria | China | Iran | Philippines |
| Australia | France | Italy | South Korea |
| Austria | Germany | Japan | Thailand |
| Bangladesh | India | Jordan | United Kingdom |
| Brazil | Indonesia | Netherlands | United States |
| Canada | Iraq | Nigeria | Yemen |

*Note: Figures as at 31 December 2018*

# Broad-based Research-Intensive University

**12 Faculties**

1. Arts & Social Sciences
2. Built Environment
3. Business & Accountancy
4. Computer Science & IT
5. Dentistry
6. Economics & Administration
7. Education
8. Engineering
9. Languages & Linguistics
10. Law
11. Medicine
12. Science

**2 Academies**

1. Islamic Studies
2. Malay Studies

**3 Academic Centres**

1. Foundation Studies
2. Sport & Exercise Sciences
3. Cultural

**3 Institutes**

1. Institute for Advance Studies (IAS)
2. Asia-Europe Institute (AEI)
3. International Institute of Public Policy and Management (INPUMA)

**4 Research Clusters**

1. Social Advancement & Happiness
2. Health & Well-Being
3. Frontiers of The Natural World
4. Innovative Industry & Sustainability Science

**~100** Undergrad Programmes

**~180** Masters Programmes

**4** Doctoral Programmes

**2** Double Degree

**8** Dual/Double Masters

**25** Joint /Dual PhDs

# UM Rankings

70

QS WORLD UNIVERSITY RANKINGS

46

THE TIMES HIGHER EDUCATION ASIA UNIVERSITY RANKINGS

19

QS UNIVERSITY RANKINGS ASIA

34

UI GreenMetric World University Ranking

# Thermoelectrics??

# Seebeck Effect

Thermoelectricity - known in physics as the "Seebeck Effect"

- In 1821, Thomas Seebeck, a German physicist, twisted two wires of different metals together and heated one end.
- Discovered a small current flow and so demonstrated that heat could be converted to electricity.

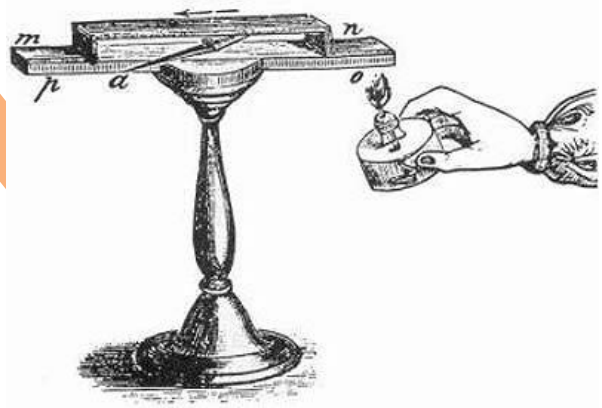


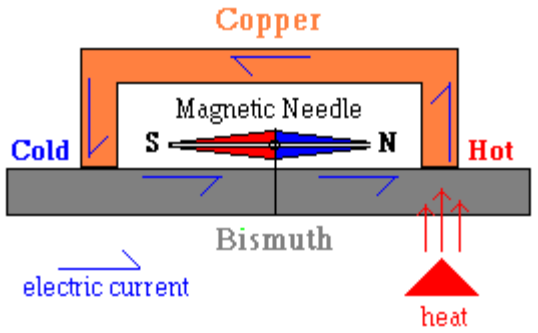

# Thermoelectric Effect

- Interconversion of electrical energy and thermal gradients in materials.
  - in a thermal gradient, an electromotive force (emf) is produced
  - a thermal gradient is induced when a current is made to flow

The more energetic electrons at the hot side (Th) of the material have a longer mean free path compared with electrons at the cold side (Tc) of the material.

These more energetic electrons (denoted by white dots) then diffuse to the cold side, which induces the development of an electric field (E) to resist further diffusion.

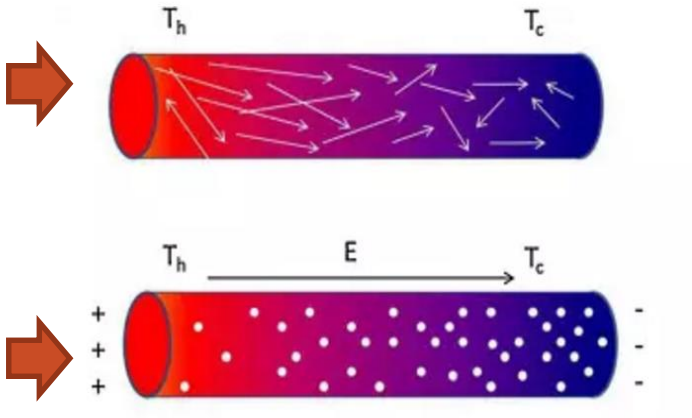


## SEEBECK EFFECT

- A temperature difference between two points in a conductor or semiconductor results in a voltage difference between these two points

- The Seebeck effect arises when charge carriers-**electrons or holes**—are excited to higher energy levels at the hot contact/sources and then diffuse throughout the material toward cooler areas.

**Seebeck Coefficient**

$$S = \frac{dV}{dT}$$

# Thermoelectric device

- Generally, most metals possess Seebeck coefficients of 10 μV/K or less, but semiconductor materials are promising in constructing the thermocouples because they have Seebeck coefficients in excess of 100 μV/K

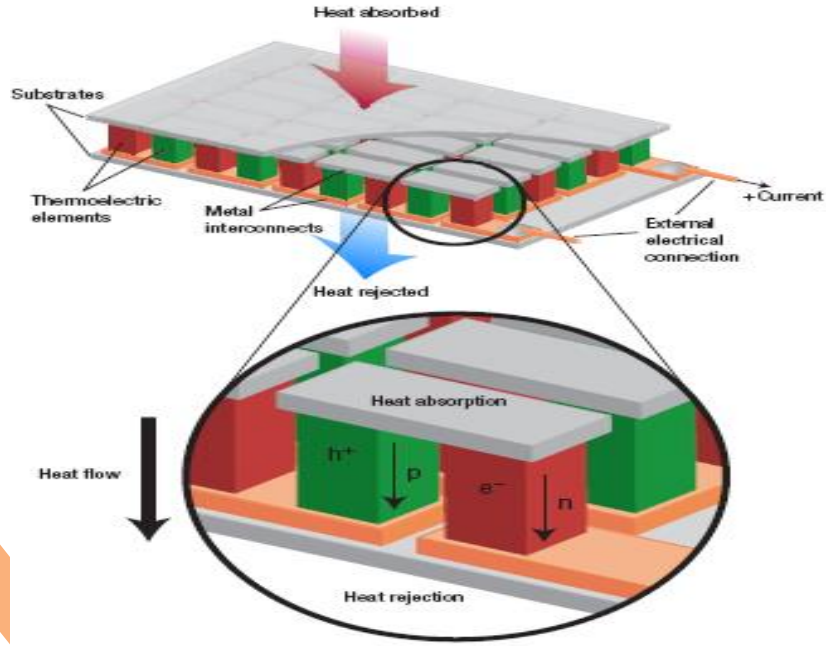


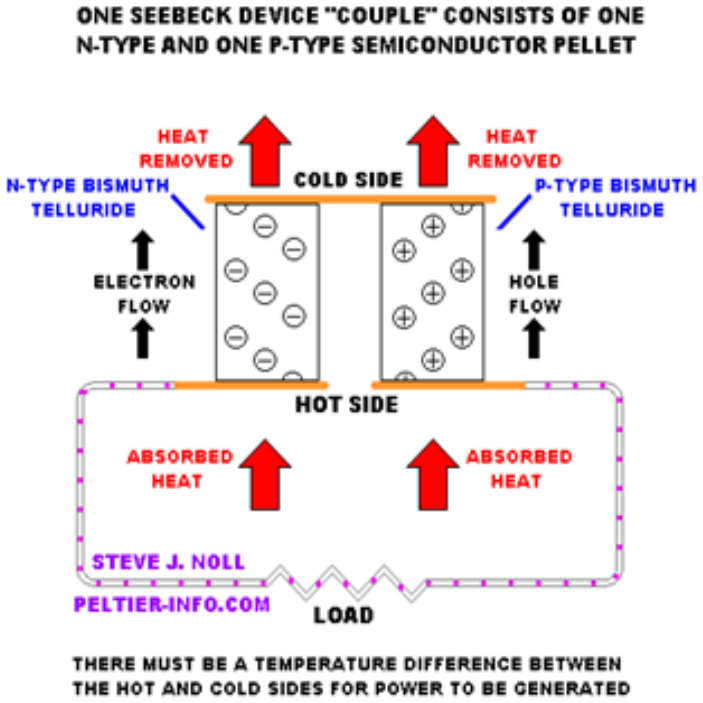


- Electron/hole pairs excited when in contact with heat sources.
- Pairs recombine and reject heat at the cold end.
- The net voltage appears across the bottom of the thermoelectric legs.

Snyder et al. *Nature* 7, 105-114, (2008). Rowe D.M., Thermoelectrics Handbook, 2006.

# Important Properties

## Figures of merit , *ZT*

- The coefficient of performance (e) for a thermoelectric power generator or cooler depends on the active thermoelectric material through:

$$ZT = \frac{\sigma S^2 T}{K}$$

$\sigma$ = Electrical Conductivity

S = Seebeck Coeffcient

$K$ = Thermal Conductivity

## Thermal Conductivity, *k*

$$\kappa = \kappa_e + \kappa_l$$

$$\kappa_e = L\sigma T = ne\mu LT$$

- *n – carrier concentration*
- *$m^*$ - effective mass of carrier*
- *μ – carrier mobility*

# Figure of Merit – Conflicting Properties

## Figure of Merit - zT

$$zT = \frac{S^2 \sigma T}{\kappa} \quad => \quad z = \frac{S^2 \sigma}{\kappa}$$

**S - Seebeck Coefficient**

$$S = \frac{8\pi^2 k_B^2}{3eh^2} m^* T \left( \frac{\pi}{3n} \right)^{2/3}$$

**σ - Electron Conductivity**

$$\sigma = \frac{1}{\rho} = ne\mu$$

**κ - Thermal Conductivity**

$$\kappa = \kappa_e + \kappa_l$$

$$\kappa_e = L\sigma T = neL\mu T$$

*n - carrier concentration*
*$m^*$ - effective mass of carrier*
*μ - carrier mobility*

## Effect of Carrier Concentration

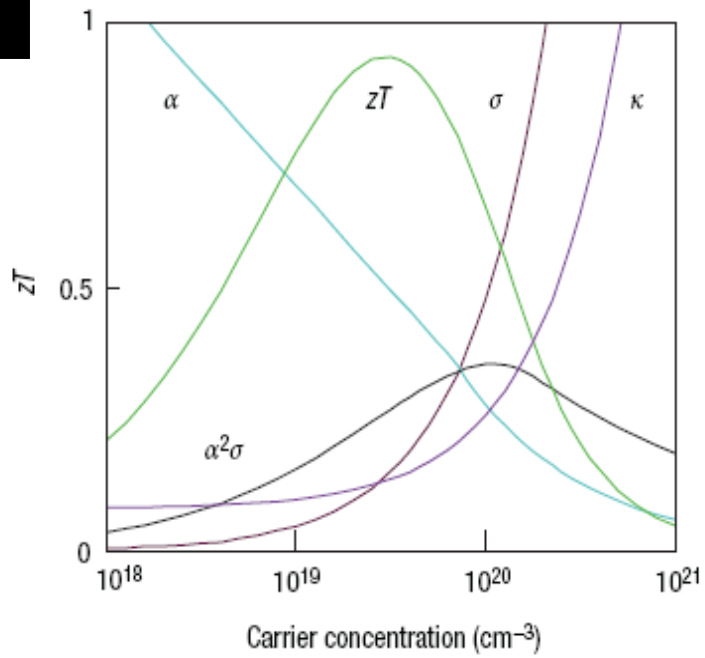


Snyder et al. *Nature* 7, 105-114, (2008).

# Figure of Merit – Conflicting Properties

## Figure of Merit - zT

$$zT = \frac{S^2 \sigma T}{\kappa} \quad => \quad z = \frac{S^2 \sigma}{\kappa}$$

**S - Seebeck Coefficient**

$$S = \frac{8\pi^2 k_B^2}{3eh^2} m^* T \left(\frac{\pi}{3n}\right)^{2/3}$$

**σ - Electron Conductivity**

$$\sigma = \frac{1}{\rho} = ne\mu$$

**κ - Thermal Conductivity**

$$\kappa = \kappa_e + \kappa_l$$

$$\kappa_e = L\sigma T = ne\mu L T$$

*n - carrier concentration*
*$m^*$ - effective mass of carrier*
*μ - carrier mobility*

## Effect of Temperature

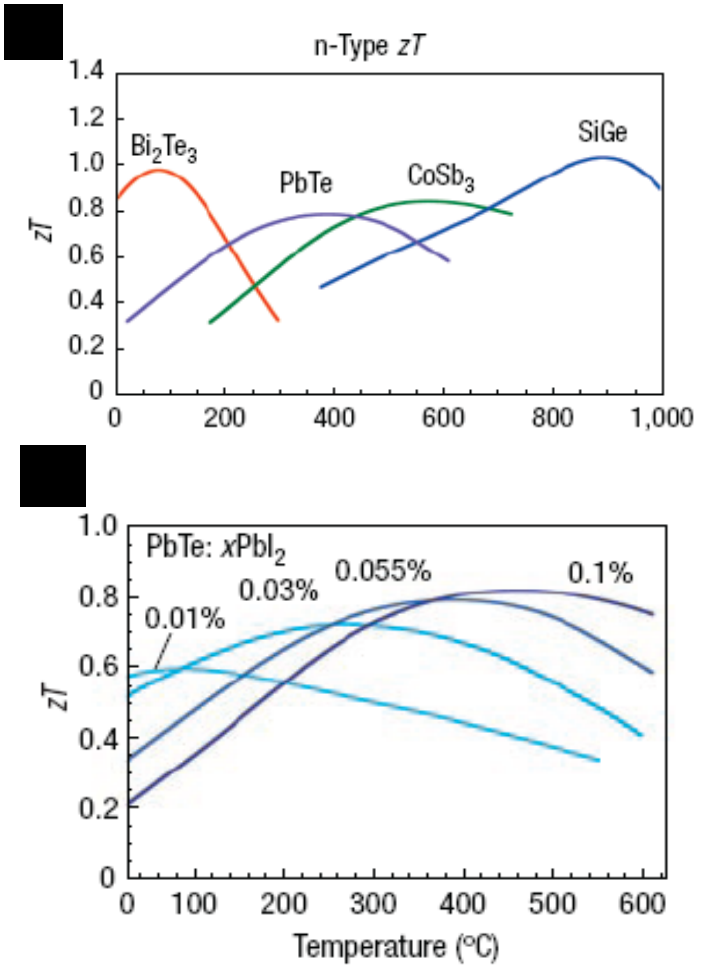


Snyder et al. *Nature* 7, 105-114, (2008).

# Figure of Merit – Conflicting Properties

## Figure of Merit - zT

$$zT = \frac{S^2 \sigma T}{\kappa} \quad => \quad z = \frac{S^2 \sigma}{\kappa}$$

**S - Seebeck Coefficient**

$$S = \frac{8\pi^2 k_B^2}{3eh^2} m^* T \left( \frac{\pi}{3n} \right)^{2/3}$$

**σ - Electron Conductivity**

$$\sigma = \frac{1}{\rho} = ne\mu$$

**κ - Thermal Conductivity**

$$\kappa = \kappa_e + \kappa_l$$

$$\kappa_e = L\sigma T = ne\mu LT$$

*n - carrier concentration*
*$m^*$ - effective mass of carrier*
*μ - carrier mobility*

- Best micro-scale materials operate at ZT = 1 (10% of Carnot efficiency)
- To run at 30% efficiency (home refrigeration) need a ZT=4.

DiSalvo, *Science*, 285 (1999)

Bell. *Science*, 321 (2008)

# TE Materials

Thermoelectric materials research is an application-driven multidisciplinary topic of fundamental research, which involves the charge, spin, orbital, and lattice degrees of freedom of material.

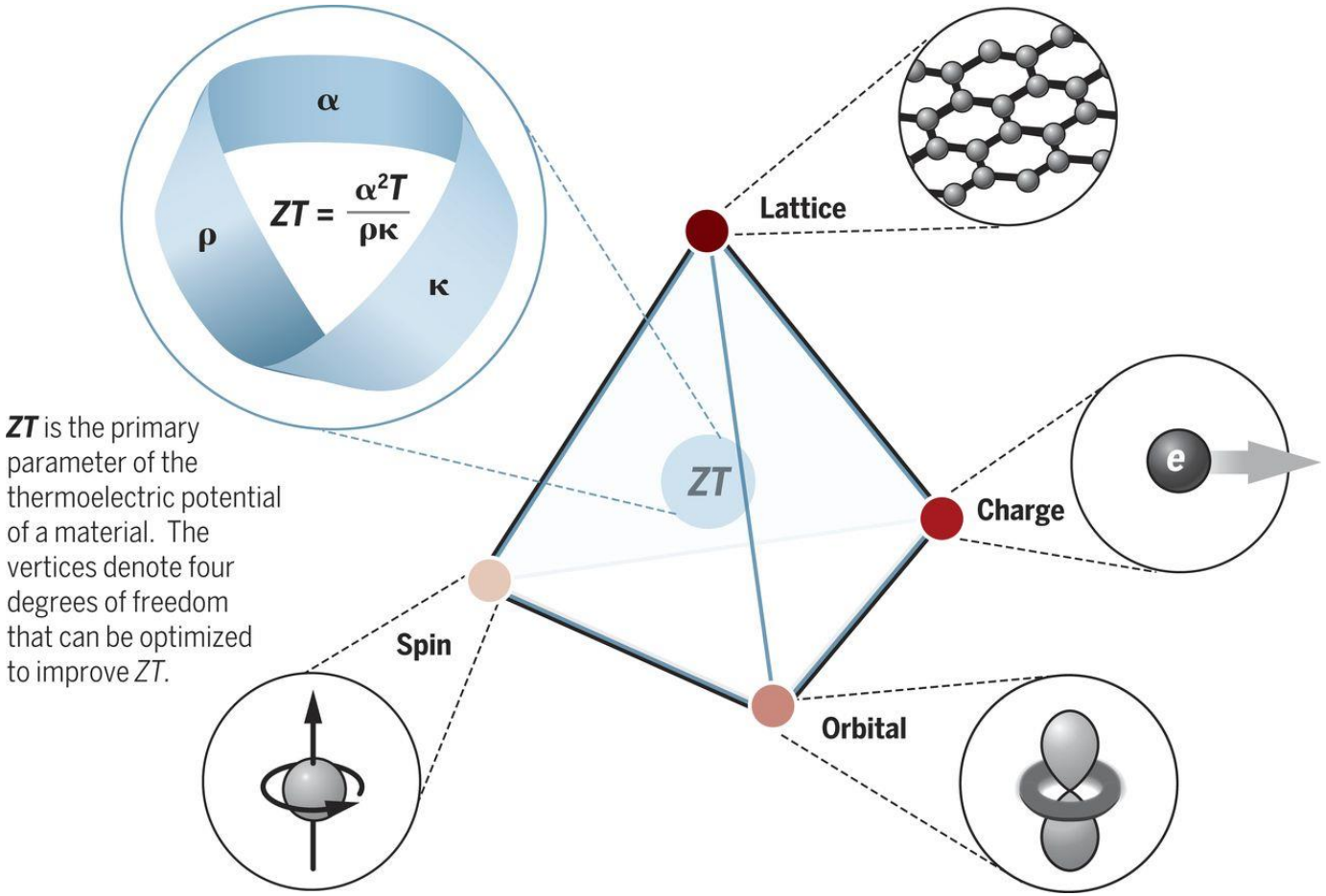


***ZT*** is the primary parameter of the thermoelectric potential of a material. The vertices denote four degrees of freedom that can be optimized to improve *ZT*.

# Materials of Choice

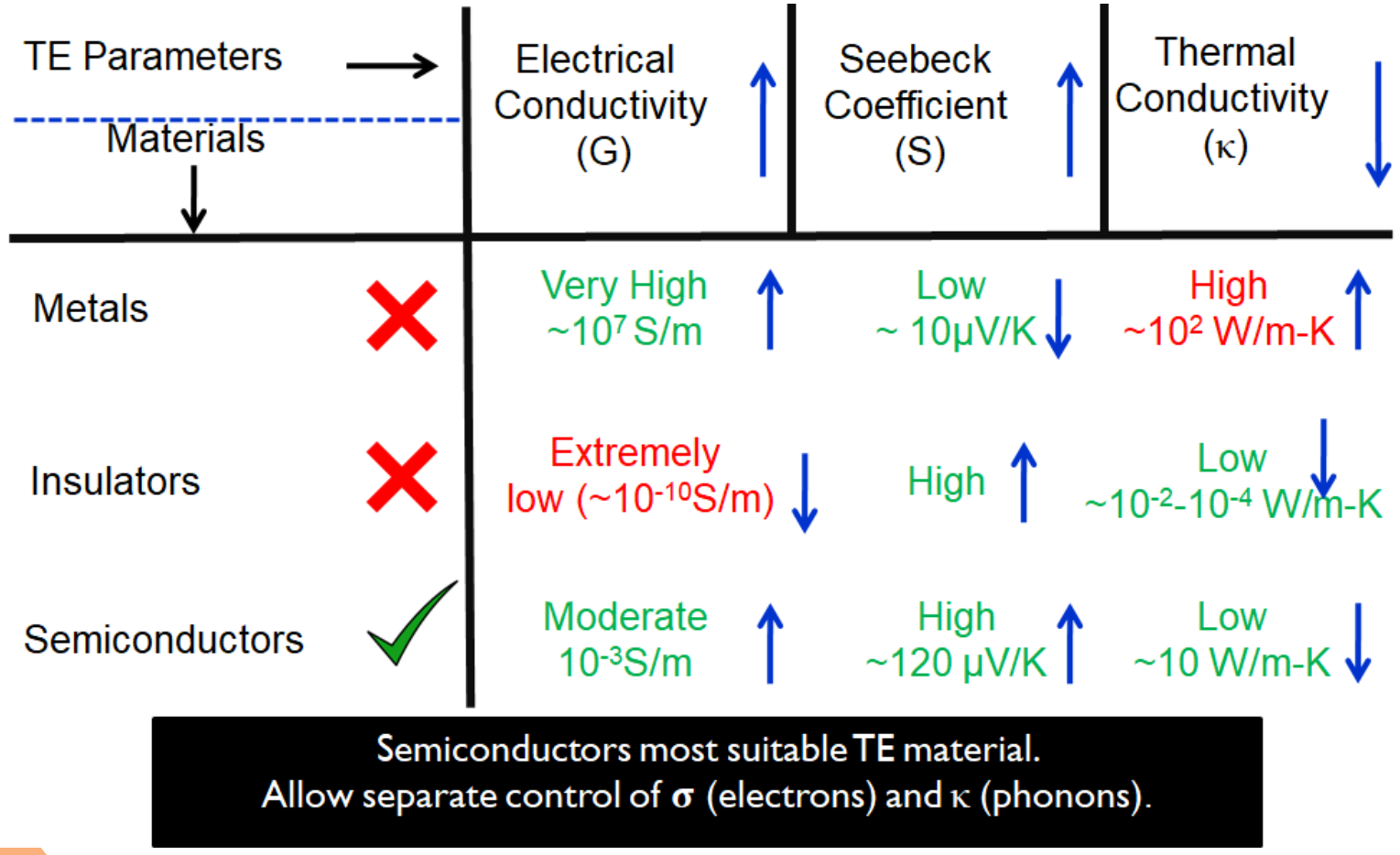


Semiconductors most suitable TE material.
Allow separate control of $\sigma$ (electrons) and $\kappa$ (phonons).

# Some TE Materials Performances

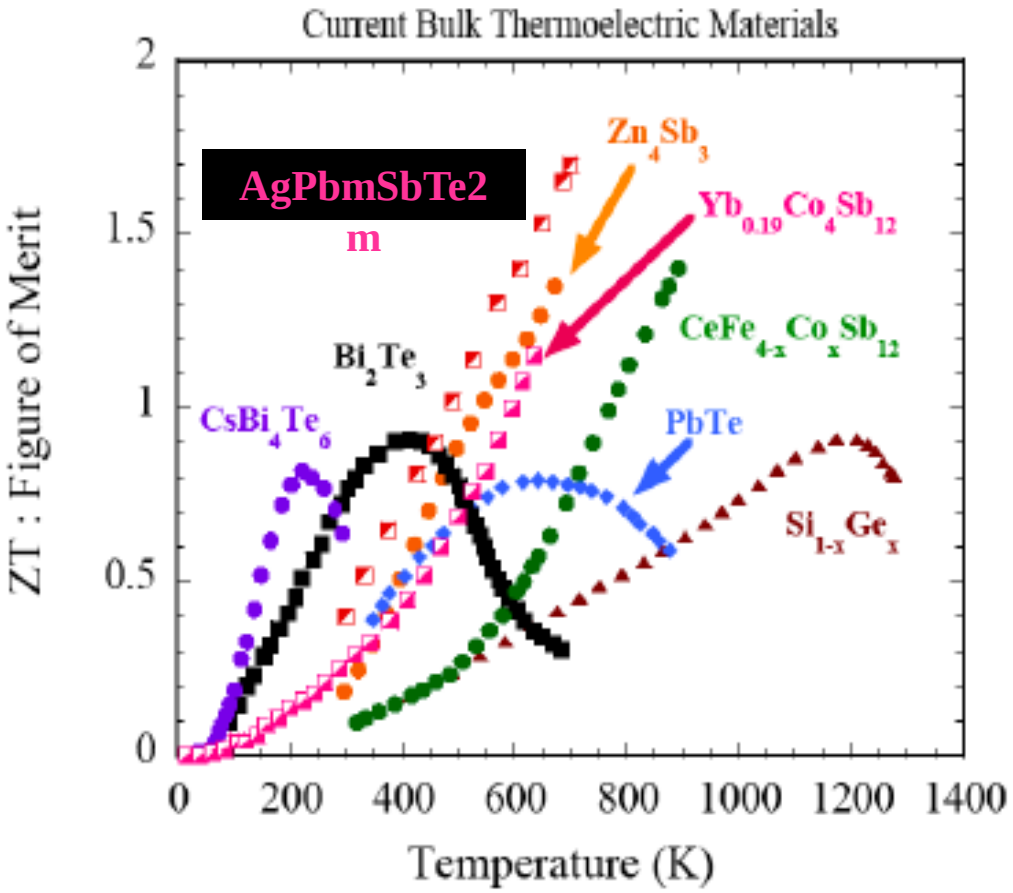


- PbTe/$Bi_2$ $Te_3$ (room to mid temperature)
- Alloy Si-Ge (high temperature)
- Mixed chalcogenides with complex structures (mid to high temperature)
- Thallium compounds (mid temperature)
- Phonon glass-electron crystals (mid to high temperature)

# Efficiency relation with ZT

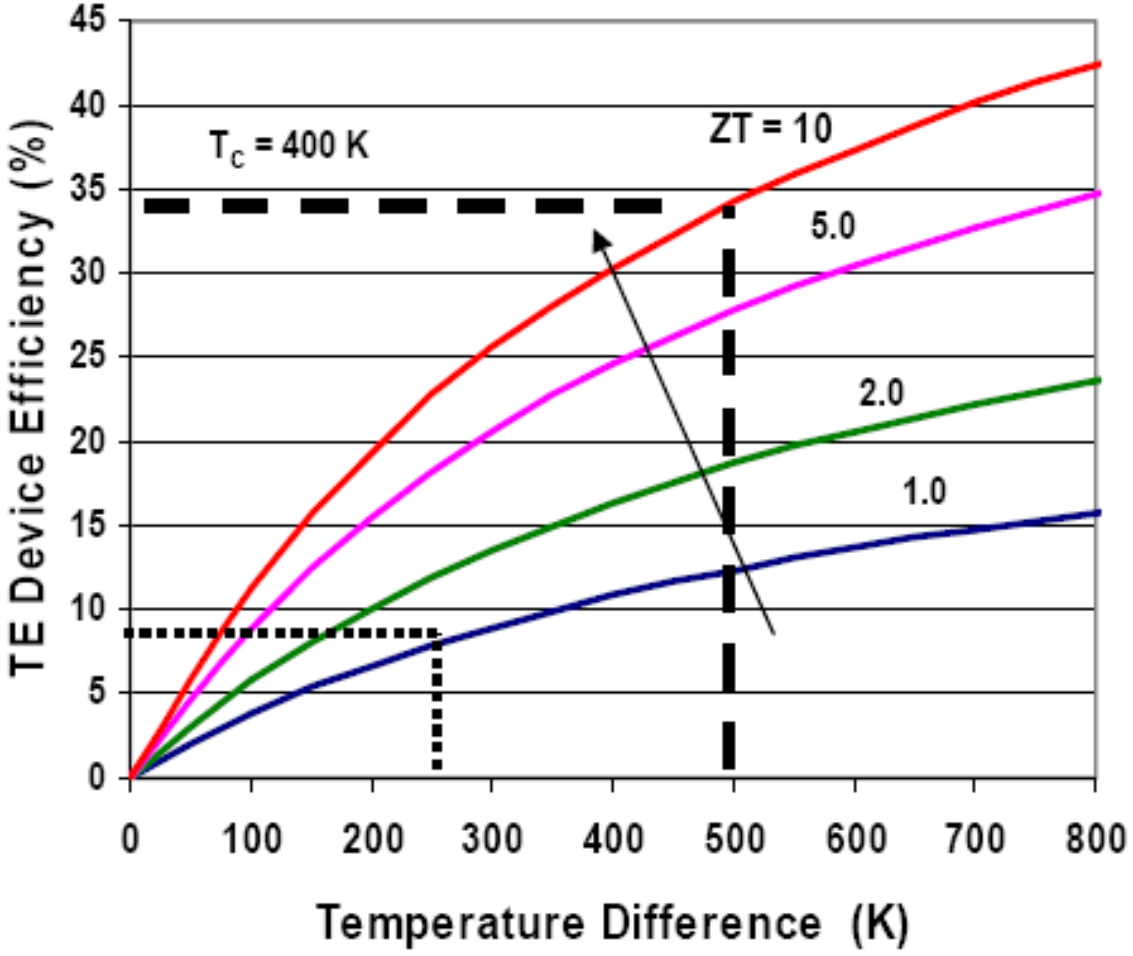

# TEG Applications Roadmap

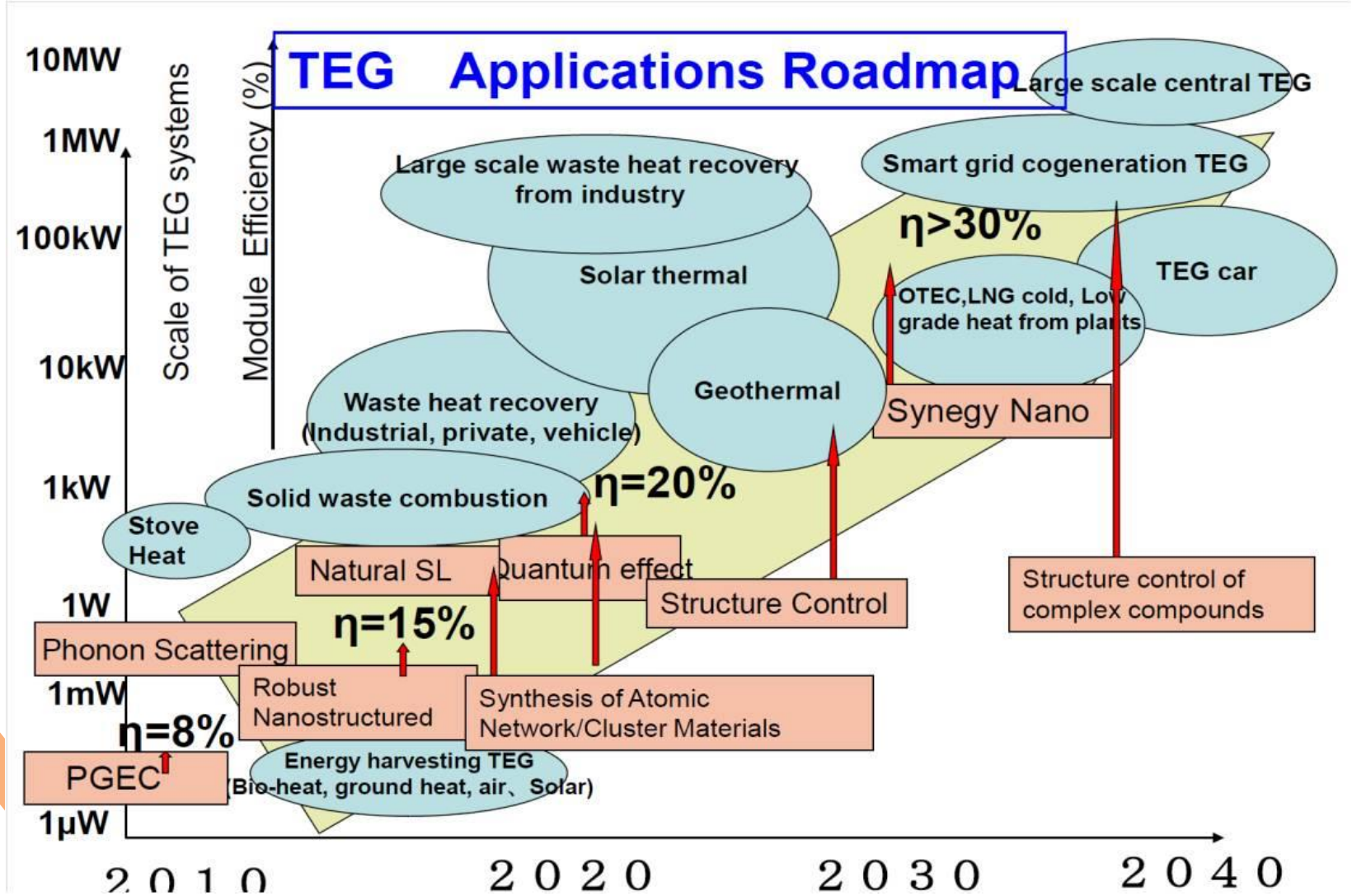

# TE Performances Progress

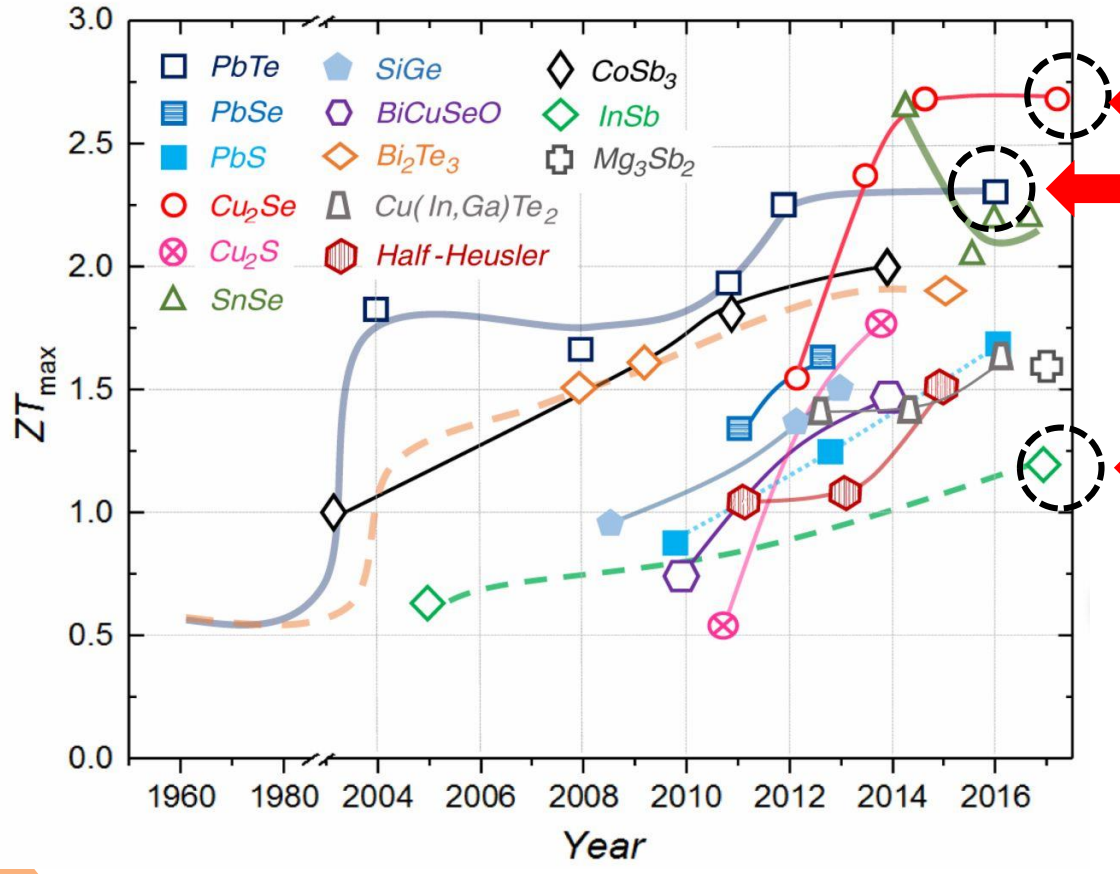


$Cu_2Se$ at ≤850K

PbTe at 820K

InSb at 773K

# WEARABLE TECHNOLOGIES

- In 1821, the thematron's technology developed watches at Centre electronique horloger (CEH) in Neuchatel, Switzerland;




- In 1988, Seiko developed a thermic watch;

# WEARABLE TECHNOLOGIES

- In 2010, Skinny Player was designed by Chinese engineers Chih-Wei Wang and Shou-His Fu


- In 2013, Fujifilm has developed the flexible polymer TE conversion module;

- 2016, Embr Wave body thermostat developed by Sam Shames

# INORGANIC MATERIALS:

## The last 5 years

| | Seebeck (μV/K) | T (°C) | ZT | P. Factor (μW/mK$^2$ ) | Thermal Conductivity (W/mK) |
|---|---|---|---|---|---|
| $AgPb_{18}SbTe_{20}$ | -370 | 527 | 2.19 | 29.57 | 1.08 |
| $AgPb_{18}SbTe_{20}$ | -335 | 427 | 1.99 | 31.42 | 1.1 |
| (Sr0.25Ba0.25Yb0.50)0.5Co4Sb12.5 | | 598 | 1.9 | | |
| $In_{0.2}Ce_{0.2}Co4Sb_{12}$ | 295 | 327 | 1.7 | 28.46 | 1 |
| PbTe–SrTe (2%) | 285 | 527 | 1.7 | 285 | 0.95 |
| Na-doped PbTe–5 mol% CaTe | 265 | 527 | 1.7 | 24.57 | 1.15 |
| $In_{0.2}Ce_{0.1}Co_4Sb_{12}$ | 340 | 327 | 1.6 | 26.58 | 1 |
| $Pb_{0.96}Mn_{0.04}Te$:Na | 263 | 427 | 1.6 | 23 | 1 |
| $AgSbTe_2$ | 242 | 377 | 1.57 | 8.6 | 0.38 |
| $(Ti_{0.30}Zr_{0.35}Hf_{0.35})_{29}Ni_{33}(Sn_{0.994}\ Sb_{0.006})_{38}$ | -275 | 427 | 1.51 | 60.5 | 2.8 |
| p-type $Bi_2Te_3$ | 225 | 117 | 1.5 | 31.64 | 0.8 |
| $Ti_{0.5}(Zr_{0.5}Hf_{0.5})_{0.5}NiSn_1YSbY$ (Y=0.002) | -280 | 527 | 1.5 | 52.21 | 2.9 |
| $AgSbSe_{0.02}Te_{1.98}$ | 250 | 327 | 1.36 | 14.06 | 0.62 |

# FLEXIBLE HYBRID TE MATERIALS:

## The last 5 years

| Device/ method and substrates | Materials | | Δ T | OCV | $P_{max}$ | Year, Author |
|---|---|---|---|---|---|---|
| | P-type | N-type | | | | |
| **Flexible TEG (flexible plastic substrate)** | SWNT/PEDOT:PSS | C60/TiS2 | 20 K | | 335 nW | 2018, Wang et al. |
| **Flexible TEG (solution casting method, polyimide substrate)** | $LiClO_4$ doped poly(ether-b-amide 12)/CNT | $LiClO_4$ doped poly(ether-b-amide 12)/CNT | 60 K | OCV: 120 mV | | 2018, Luo et al. |
| **Flexible TEG (inkjet printing method, 25 m thick polyimide substrate)** | PEDOT:PSS/Ag | | 5 K | OCV ~50 V | ~0.24 pW | 2017, Beretta et al. |
| **Flexible and foldable standard paper based TE generator (micromachining and microfabrication method)** | $Sb_2Te_3$ | $Bi_2Te_3$ | 75 K | OCV: 190.7 mV | ~24 nW | 2017, Rojas et al. |
| **Wearable TEG (Welded method, flexible printed circuit board substrate)** | $Bi_2Te_3$-based TE materials | $Bi_2Te_3$-based TE materials | 12 K | Output voltage: 48 mV | 8.3 W (0.67 W/cm2) at ΔT = 11K | 2017, Liu et al. |

# FLEXIBLE HYBRID TE MATERIALS:

## The last 5 years

| Device/ method and substrates | Materials | | Δ T | OCV | $P_{max}$ | Year, Author |
|---|---|---|---|---|---|---|
| | P-type | N-type | | | | |
| **Flexible rolled TEG (screen printing method, Kapton substrate)** | PEDOT:PSS | Nickel | 65K | OCV: 260 mV | 46 W | 2017, Fang et al. |
| **Flexible TEG (drop casting method, 2 µm thick polyethylene terephthalate substrate)** | SWCNTs | SWCNTs | 27.5K | OCV: 11.3 mV | 2.51 W (167 W/cm2) | 2017, Zhou et al |
| **Silk fabric-based TEG (repeatedly depositing)** | $Sb_2Te_3$ | $Bi_2Te_3$ | 35 K | OCV: ~10 mV | ~15 nW | 2016, Lu et al. |
| **Flexible TEG (dispense-printing, polyimide substrate** | PEDOT:PSS SV3 (Ag paste) | | 90 K | Output voltage: ~25 mV | ~100 nW | 2016, Stepien et al. |
| **Free-standing flexible TE foil (solution-based synthesis process)** | | $TiS_2HA_{0.01}NMF_{0.003}$ | 20 K | OCV: ~1.3 mV | 24 nW (32 W/cm2) | 2016, Wan et al |
| **Wearable TEG** | $Bi_2Te_3$ | $Bi_2Te_3$ | | | 20 W/cm2 | 2016, Hyland et al. |
| **Polyester-based fabric TEG (solution coating, polyester fabric substrate)** | PEDOT:PSS coated polyester fabric strips connected with silver wire | | 75.2 K | OCV: 4.3 mV | 12.29 nW | 2015, Du et al. |

# FLEXIBLE HYBRID TE MATERIALS: Fabrication processes

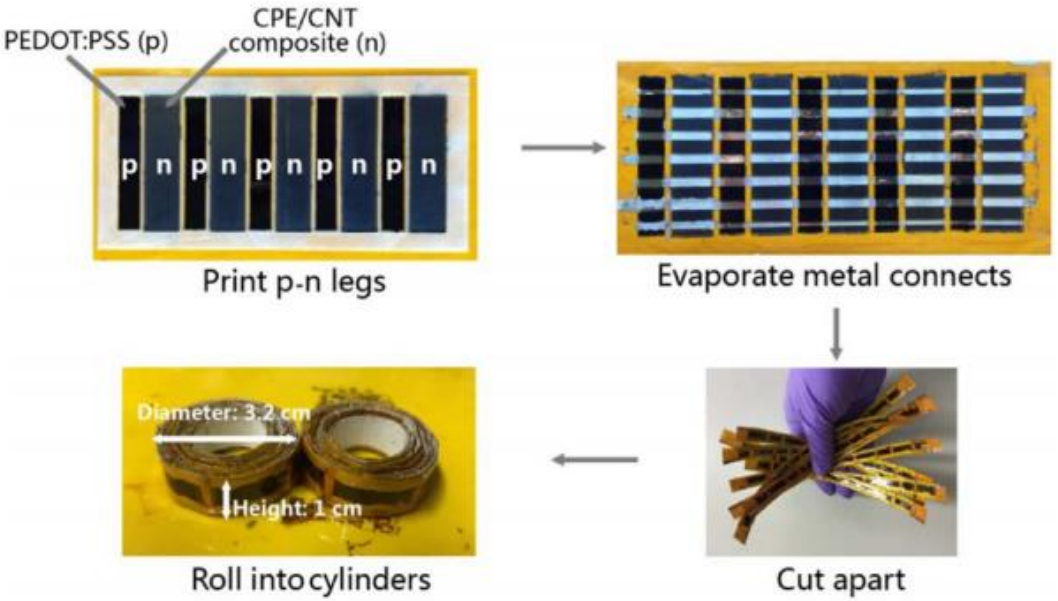


Typical fabrication process for the rolled modules using PEDOT:PSS as p-type and CPE/CNT nanocomposite as n-type legs, respectively. (Fang et al., 2017. J. Appl. Polym. Sci. 134, 44208.)

# FLEXIBLE HYBRID TE MATERIALS: Fabrication processes

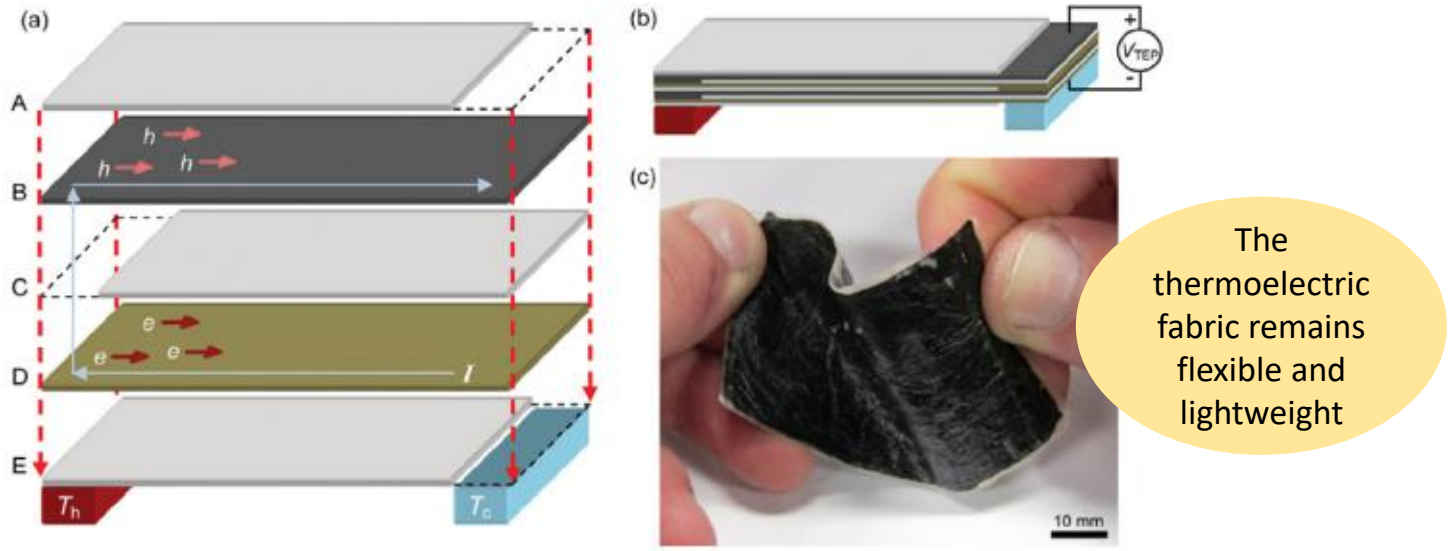


The thermoelectric fabric remains flexible and lightweight

(a) Layer arrangement for the multilayered fabric. CNT/PVDF conduction layers (B and D) are alternated between PVDF insulation layers (A, C, and E). Every other conduction layer contains p-type CNTs (B), while the others contain n-type CNTs (D).

Hewitt et al., Lett. 12 (2012) 1307–1310.

# FLEXIBLE HYBRID TE MATERIALS: Fabrication processes

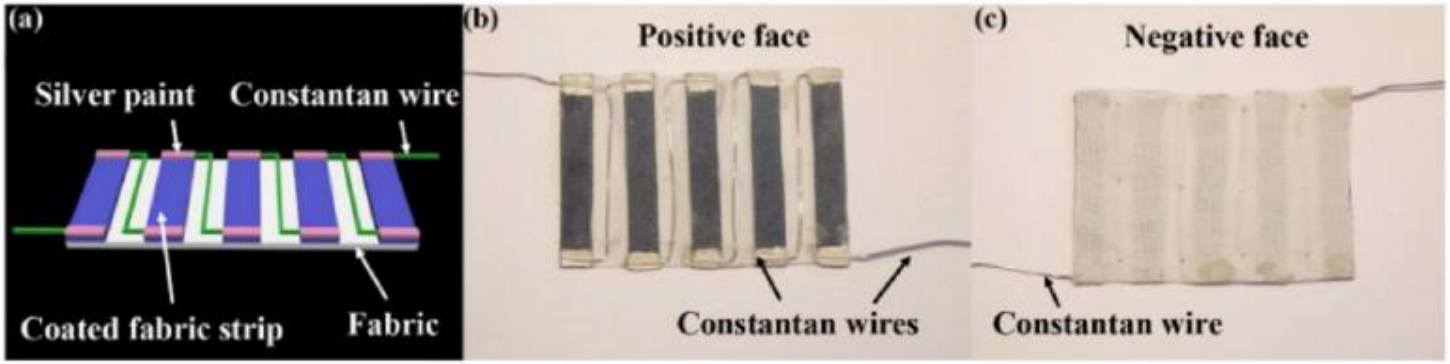


(a) Schematic illustration of the fabric-based TE generators Positive (b) and negative face (c) of the 5-strip fabric-based TE generators connected with Constantan wires.

Du et al., 2017.RSC Adv. 7,43737–43742.

# APPLICATIONS:
## Combustion drive vehicle

TEG in Porsche exhaust (944 model)

Hi-Z technology integrated TEG capable of generating 200 W (1991)

TEG tested in truck reached 1068 W electric energy

Hybrid phase (generate electric power and charging the battery)

TEG generate between 300 to 330 W electric and capable of charging 12 & 24 V

(Hi-Z technology, 2004)

BMW 5 series of 3000cc generate 500 W, $\Delta T$=207 °C)

[BSST, BMW, Visteon and Marlow Industries 2005]

Thermoelectric generator in a BMW

# APPLICATIONS: TEG mechanism in hybrid automobile

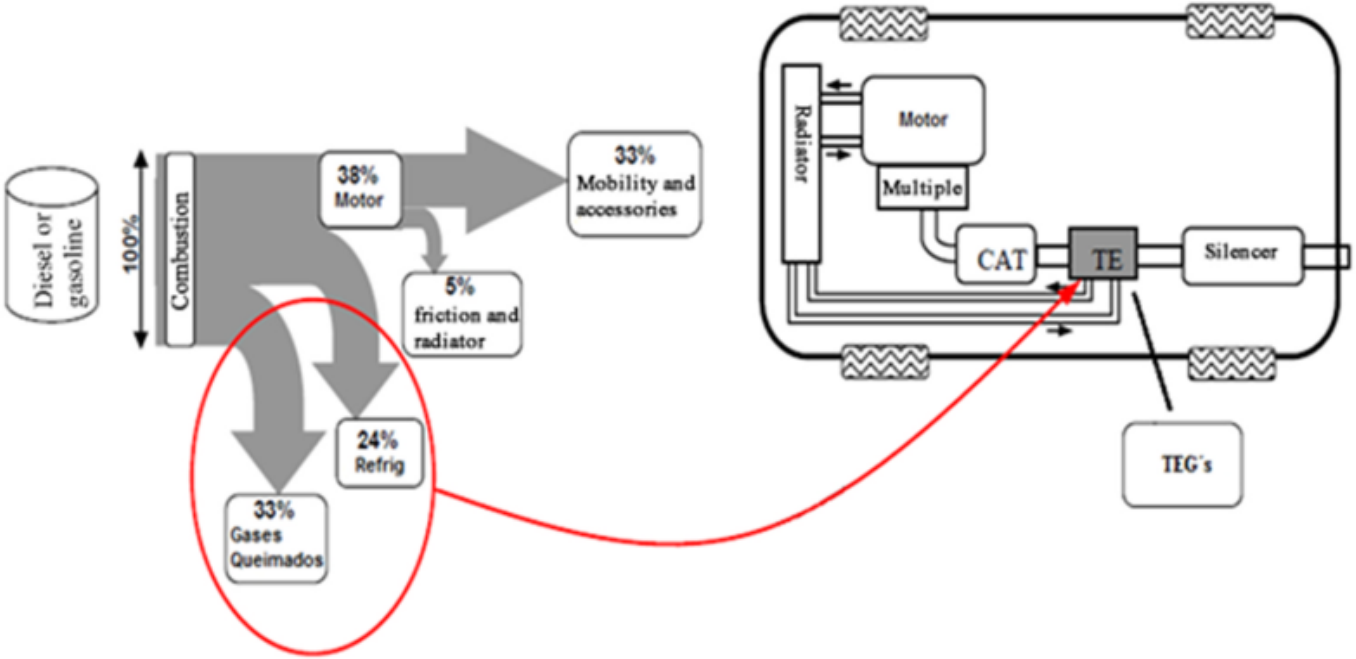


Distribution of the combustion energy in automobile

- Some studies indicate that using thermoelectric converters with an efficiency of 5% would increase the electric energy in a car by 6%
- In the United States, it is intended in 2020 to have 90% of cars with thermoelectric generators for internal cooling systems, and thus to replace air conditioners. This would save about 5% of the country's current daily average gasoline consumption and reduce greenhouse gas emissions

# APPLICATIONS: Aerospace Industry

TE modules in Voyager I by NASA. Radioisotopes TEG (RTG) , nuclear batteries convert heat into electricity.

(1977)

RTG thermocouples use natural decomposition of radioactive plutonium-238 as a source of heat and use cold outer space to produce a low T at the junction of thermocouple

Demonstration of RTG of the Voyager

https://rps.nasa.gov/

# APPLICATIONS: A new model of RTG is the MultiMission Radioisotope Thermoelectric Generator (MMRTG)

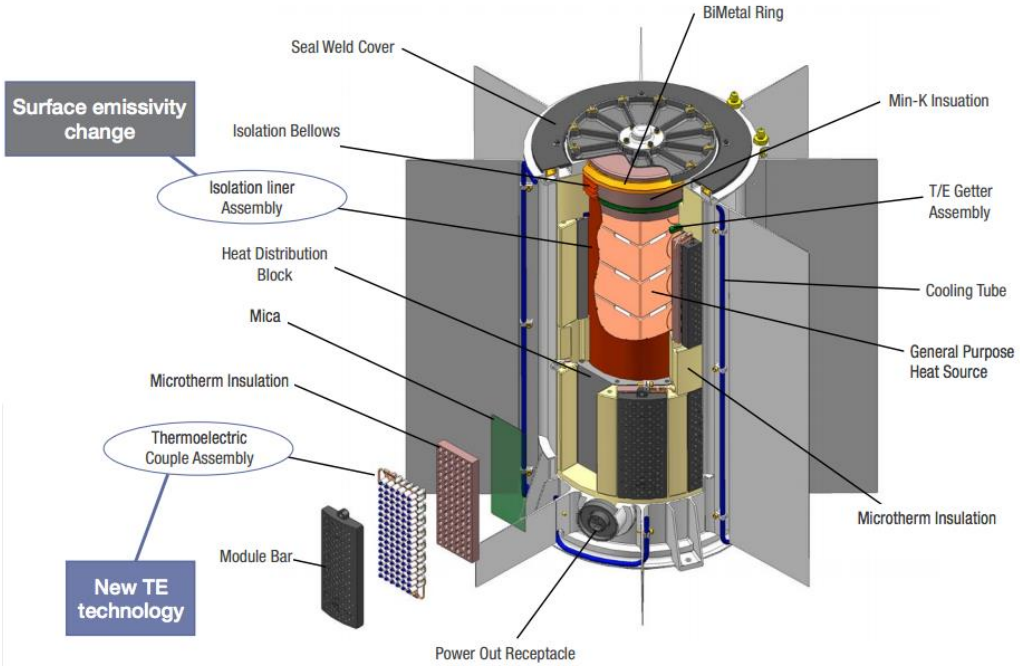


https://rps.nasa.gov/

- designed to operate on planetary bodies with atmospheres like Mars as well as in space vacuum
- Flexible and capable to generate electricity in small increments, quickly reaching 100 W
- a heat source composed of eight modules with General Purpose Heat Source
- of 4.8 kg (10.6 lb.) of plutonium dioxide which initially supplies about 2000 W of thermal power and 120 W of electrical power

# APPLICATIONS: Residential facilities

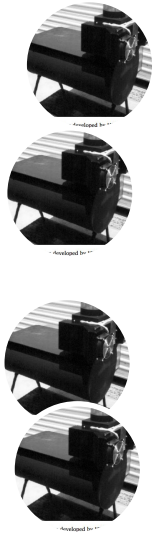

- Hi-Z technology (2002) able to generate 20 W with output voltage of 12-14 V
- The hottest area of the stove is at the top of the furnace and the cooler region is below the ash
- The best location for the thermoelectric module would be near the upper right corner next to the stove, where it will allow the highest temperature gradient
- The measured open circuit voltage, **a single module provides the highest output of 4.2 ± 0.08 W**

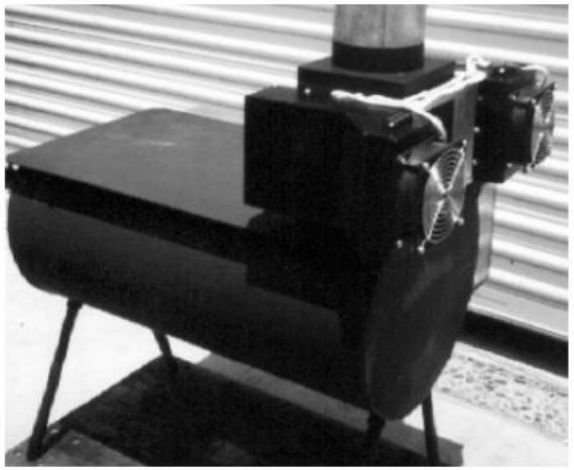

Woodstove developed by Hi-Z technology

The modules were thermoset coated at both ends and placed in the middle of an aluminum plate with the pressure applied thereto by means of a heat sink, which was held in place by an adjustable fastening mechanism

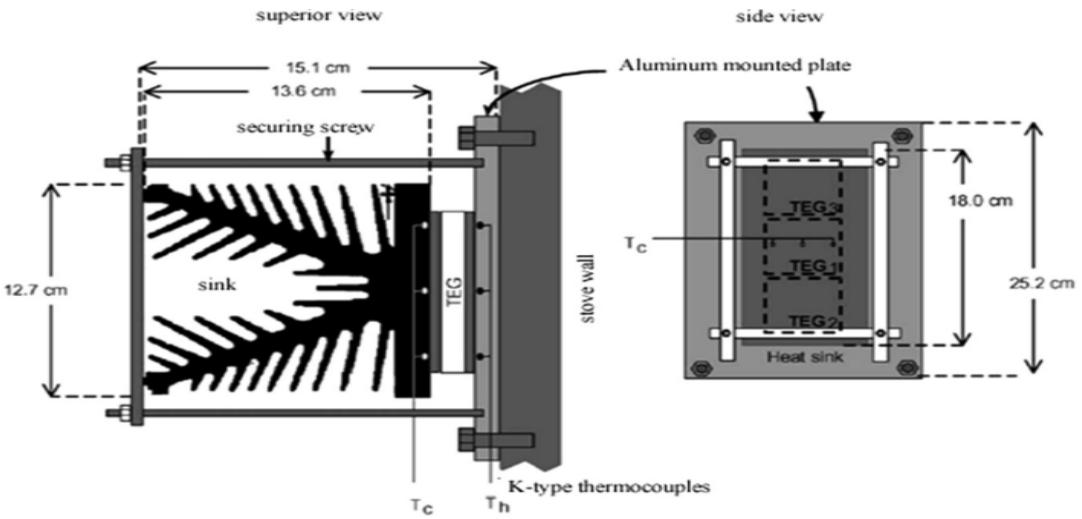


Way of fixing the thermoelectric modules on the wall

# APPLICATIONS: Building & Industrial

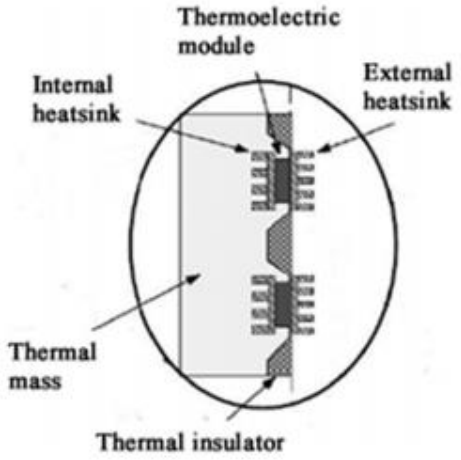


Scheme of a thermoelectric module on the wall

- The model of a device for industrial heat recovery, where the residual heat is absorbed by the heating collection block.
- The modules are fixed to the outside of the device, exposed to a hot side and a cold side.

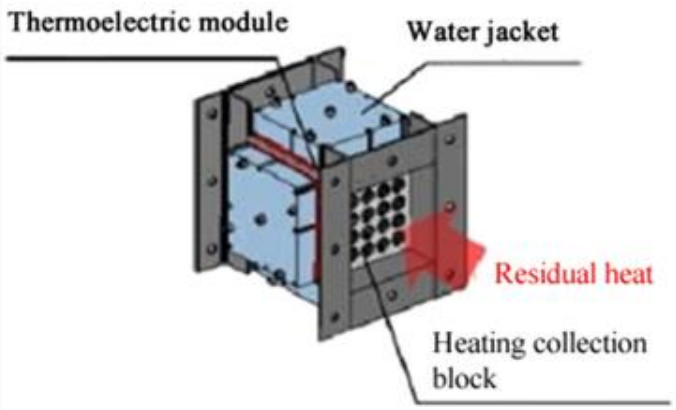


Device for heat recuperation in an industry

TEG in commercial rooms. The temperature difference is due to the outside temperature in relation to the interior, roughly 18 ° C

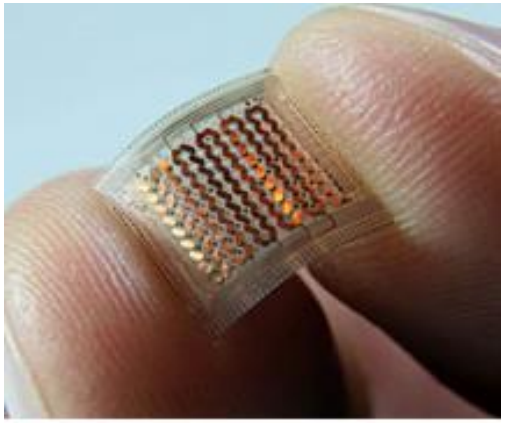

Demonstration of the GreenTEG

Green TEG, no moving parts, does not require burning fuels to generate powers

# APPLICATIONS: Portable equipment

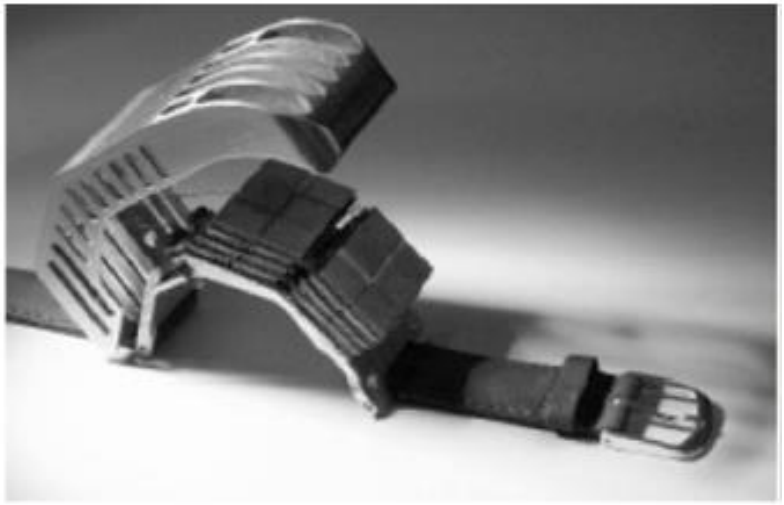

TEG for network of body sensors. $Bi_2Te_3$ in the system was able to store an average power of 100 µW on the battery and 2.4 V of output voltage. [Gyselinckx's group]

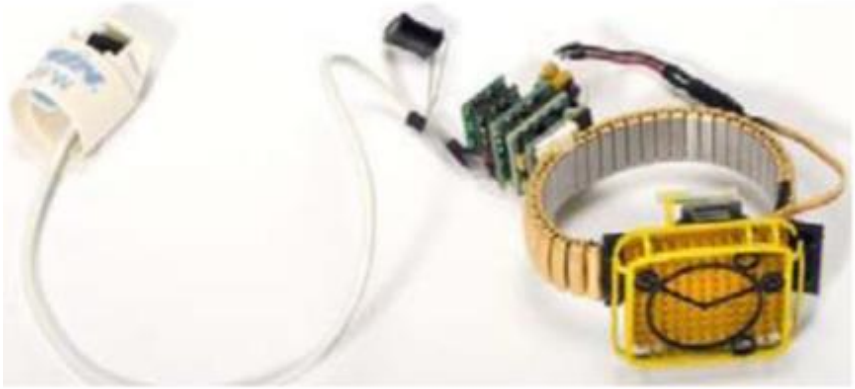

Oxímeter

- a wireless pulse oximeter by J. Penders group, powered by a pulse-type generator and also a wireless monitoring system .
- The power is 30 µW/cm2 for a voltage greater than 4 V when positioned on the wrist

# Design & Development

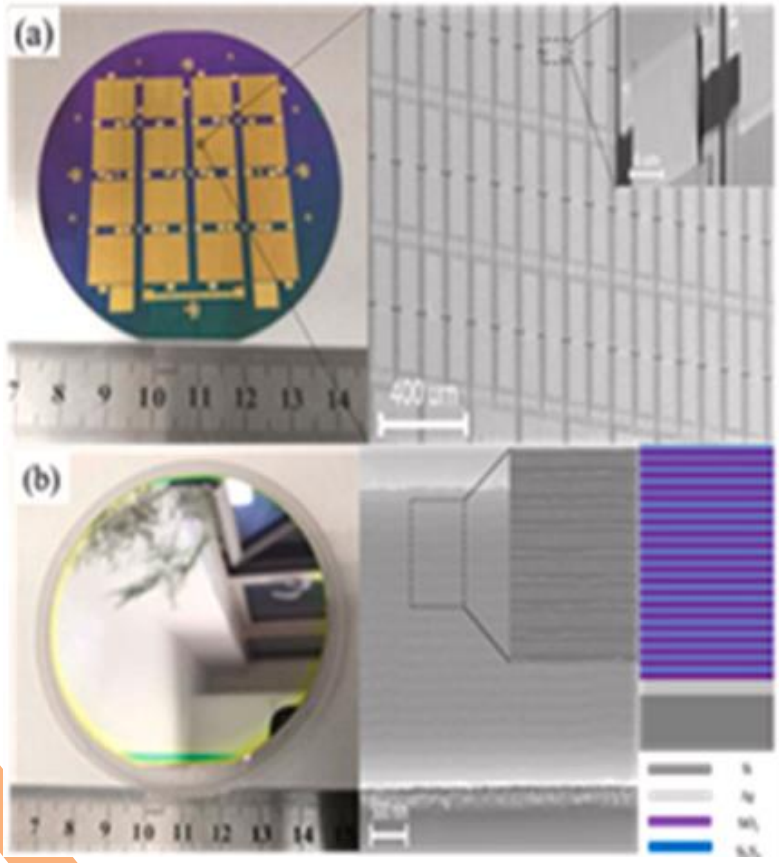


***A Novel Self-Powering Ultrathin TEG Device Based on Micro/nano Emitter for Radiative Cooling (2018)***

A highly integrated ultrathin TEG-RC can output voltage continuously TEG-RC exhibited a continuous average 0.18 mV output for 24 hours

# Design & Development

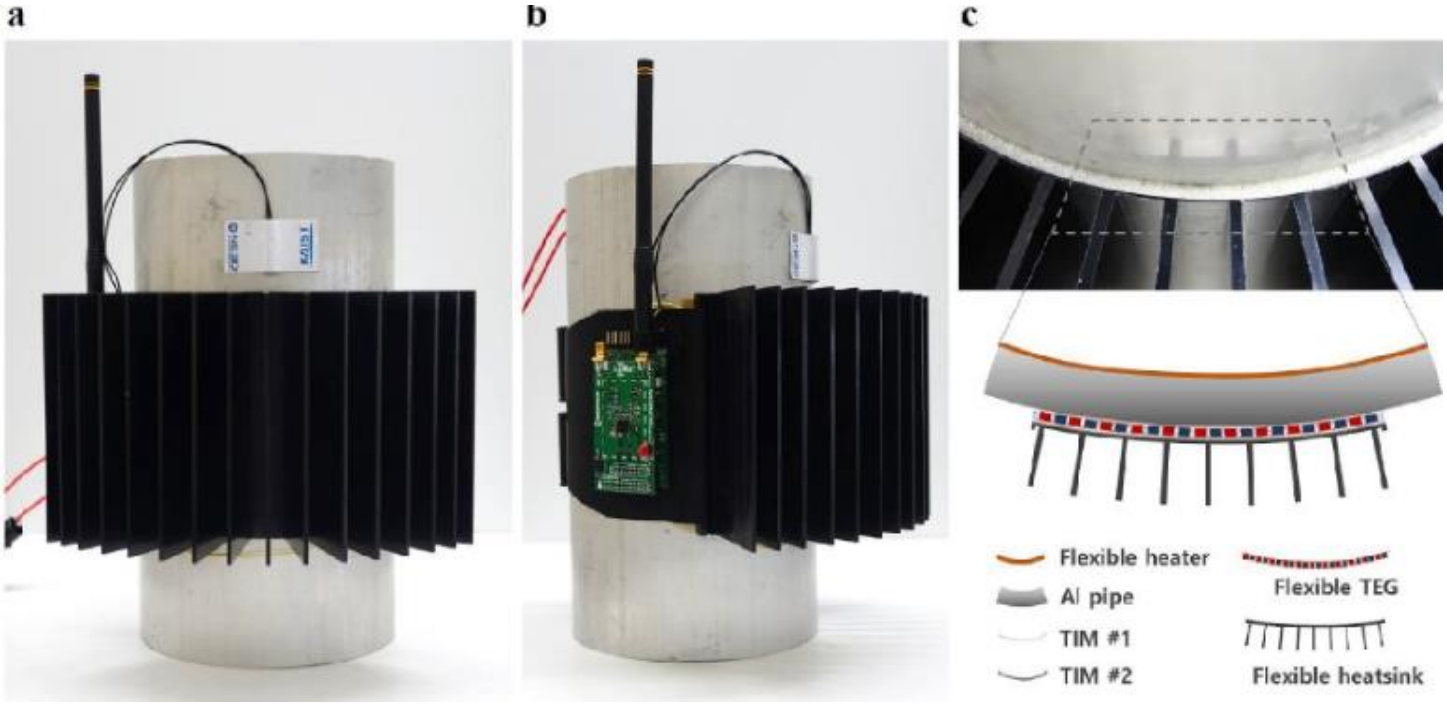


***High-performance self-powered wireless sensor node driven by a flexible thermoelectric generator (2018)***

flexible-TEG for a particular wireless sensor application, harvested 272 mW of energy from a heat pipe at a temperature of 70 °C

# Design & Development

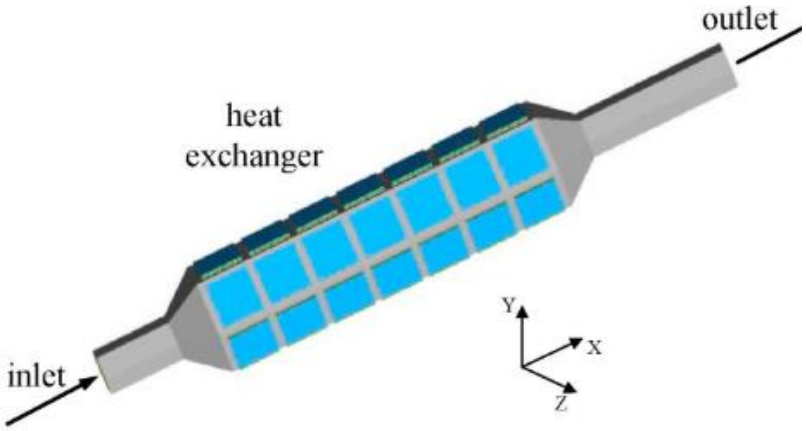


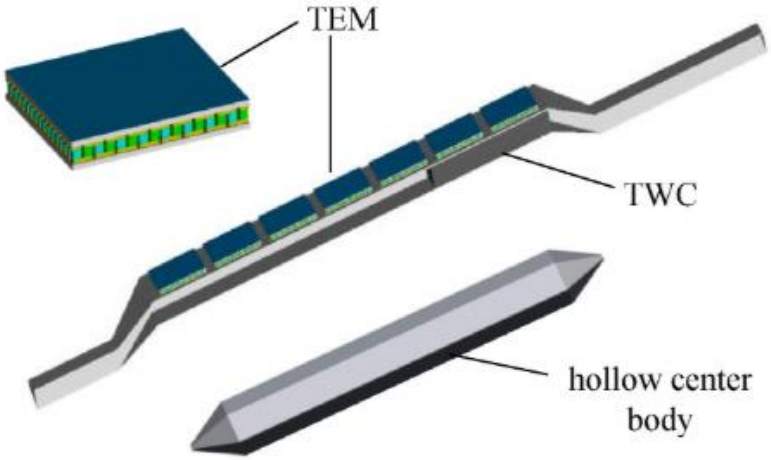


***Optimization of thermoelectric generator (TEG) integrated with three-way catalytic converter (TWC) for harvesting engine's exhaust waste heat (2018)***

A novel design of TEG integrated with TWC.

On the condition of maintaining high conversion efficiency of TWC, a moderate height of hollow center body contributes to higher maximum output power of TEG with reasonable pressure drop. Compared with a single TEG, the maximum output power of present TEG is increased by 16%, and the maximum net output power is increased by 37% with considering the power loss caused by the additional pressure drop and increased weight.

# Design & Development

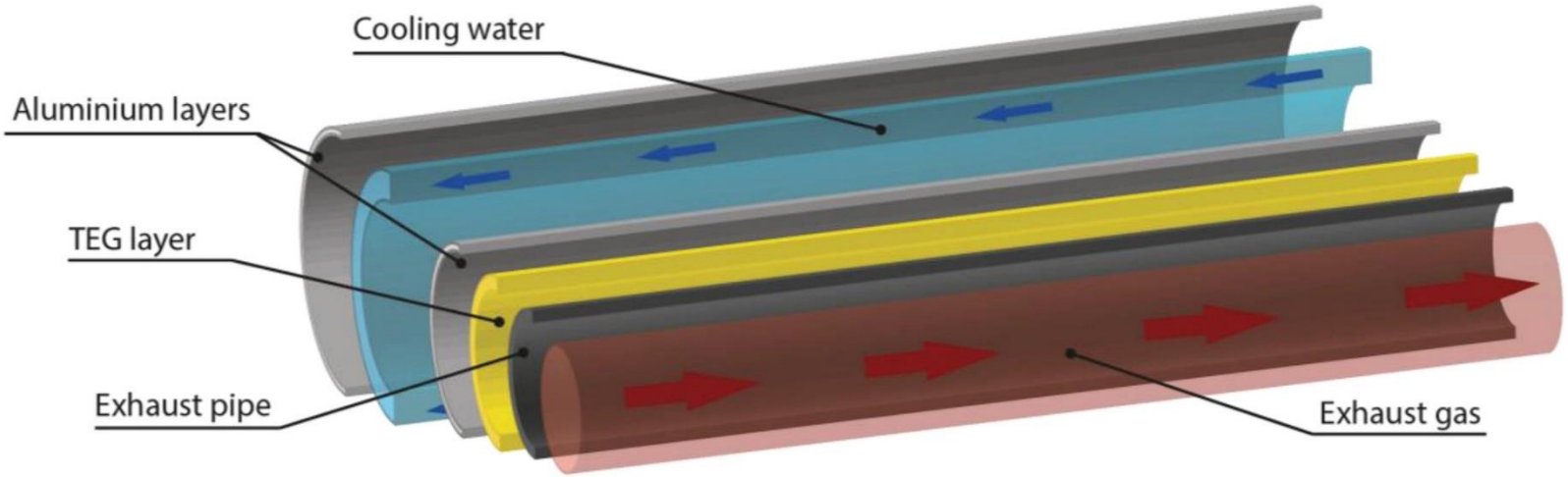


- ***Evaluating thermoelectric modules in diesel exhaust systems: potential under urban and extra-urban driving conditions (2018)***

**-***TEG applied to light duty diesel engines* working under like urban and extra-urban driving conditions

# TE MATERIALS

2016

Quarternary alloys of $Pb_{1-x}Mg_xTe_{0.8}Se_{0.2}$

ZT values as high as 2.2 can be achieved at 820K

Large size bulk materials and TE performance

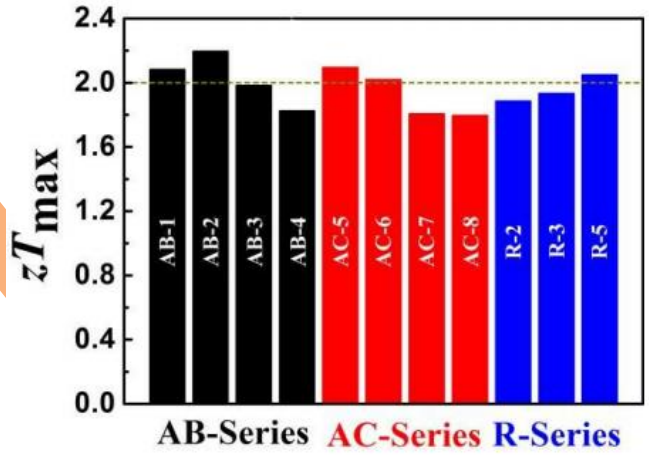


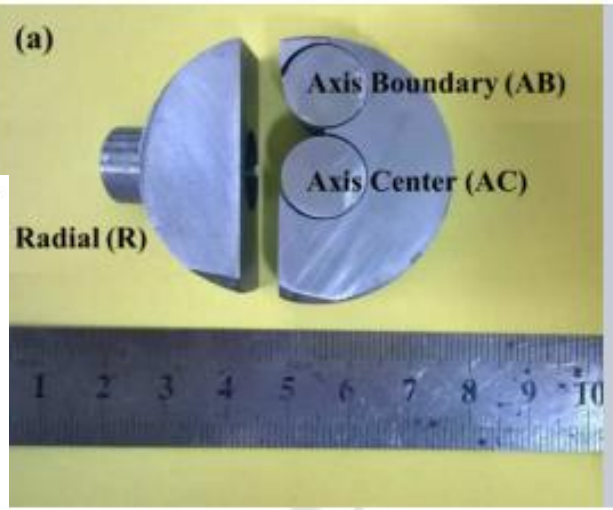


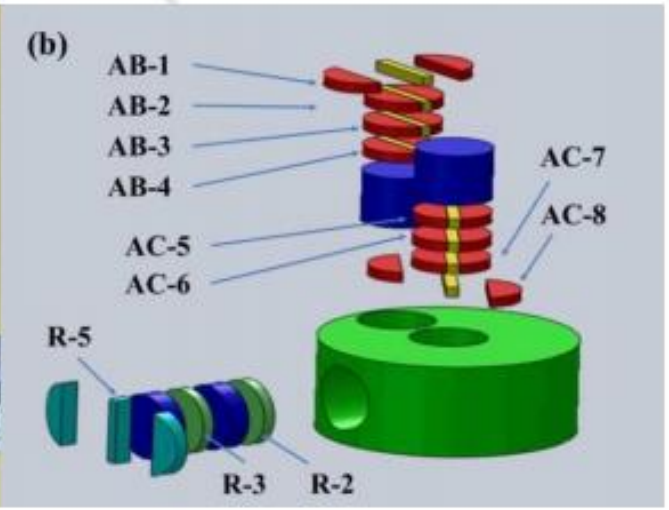


Fu et al. (2016). J. Materiomics **2**, 141–149.

2017

# ZT of 1.28 at 773K InSb-based material

- By addition of excess Sb into the InSb matrix, an InSb-Sb eutectic structure has been introduced.
- ZT value increases almost 3 times in comparison with the eutectic-free matrix.

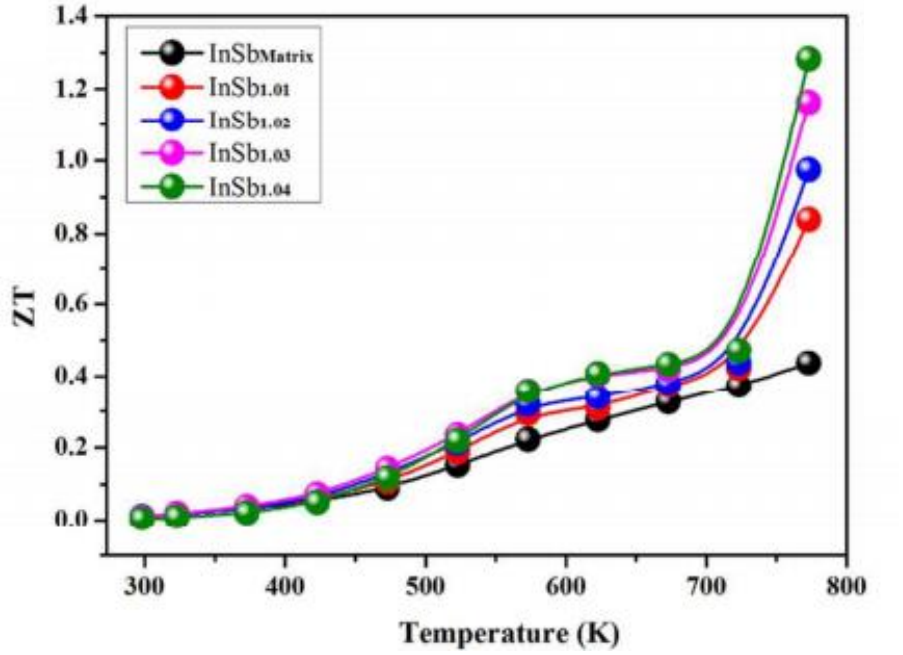


Cheng et al. (2017). J. Mater. Chem. A Mater. Energy Sustain. **5**, 5163–5170 (2017).

# TE MATERIALS

2017

ZT values as high as 2.6 can be achieved at temperatures ≤850K

View Article Online
DOI: 10.1039/C7EE01193H

Schematic illustration of the solid-state transformation of the $CuSe_2$ template into **(1-x)$Cu_2Se$/(x)$CuInSe_2$** nanocomposites.

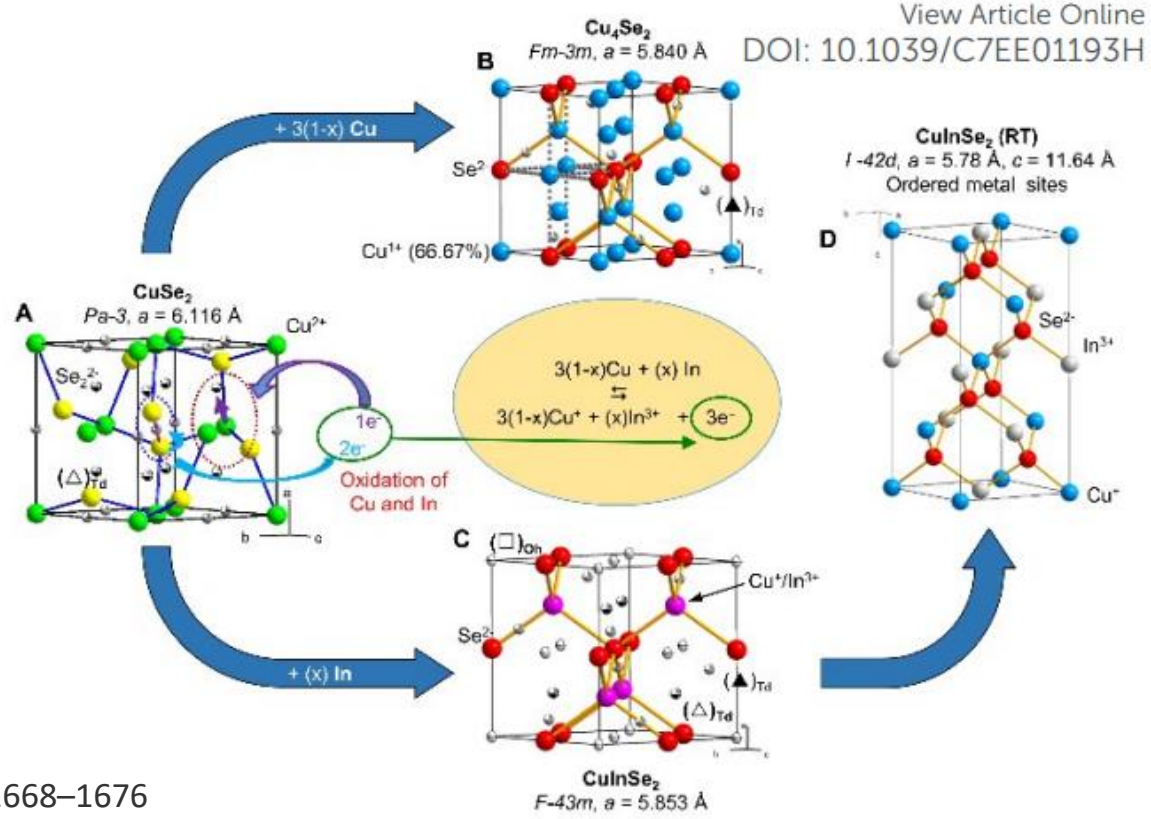


Olvera et al. (2017)Energy Environ. Sci. **10**, 1668–1676

# TE MATERIALS: Recent Development

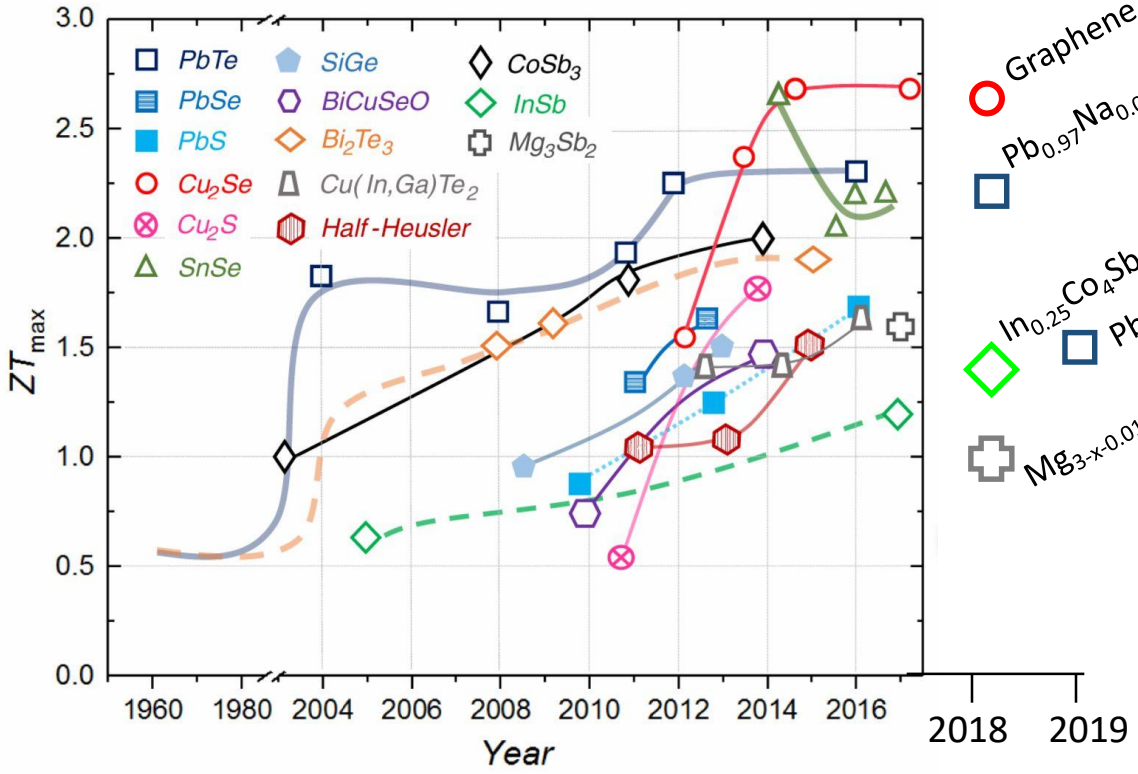


Graphene/$Cu_2Se$ at 870K

$Pb_{0.97}Na_{0.03}Te$–1 mol % $Ba_{0.5}Ca_{0.5}Te$

$In_{0.25}Co_4Sb_{12}$

$Pb_{14}Sn_4Ag_2Te_{20}$

$Mg_{3-x-0.0125}Zn_xNa_{0.0125}Sb_2$

# Research at the Lab

# Skutterudite Structure

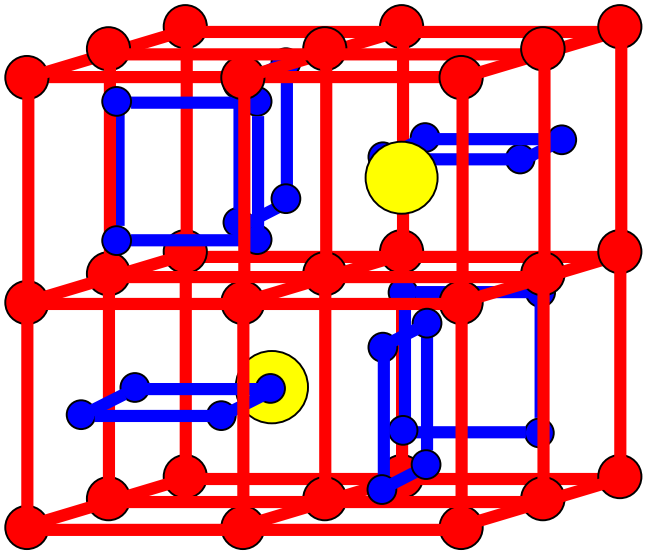

- $N_2M_8Pn_{24}$
- or $NM_4Pn_{12}$

Metal Atom (Mn, Tc, Re, Fe, Ru, Os, Co, Rh, Ir)

Pnicogen Atom (P, As, Sb)

Void Space/Filler Ion

# Methodology

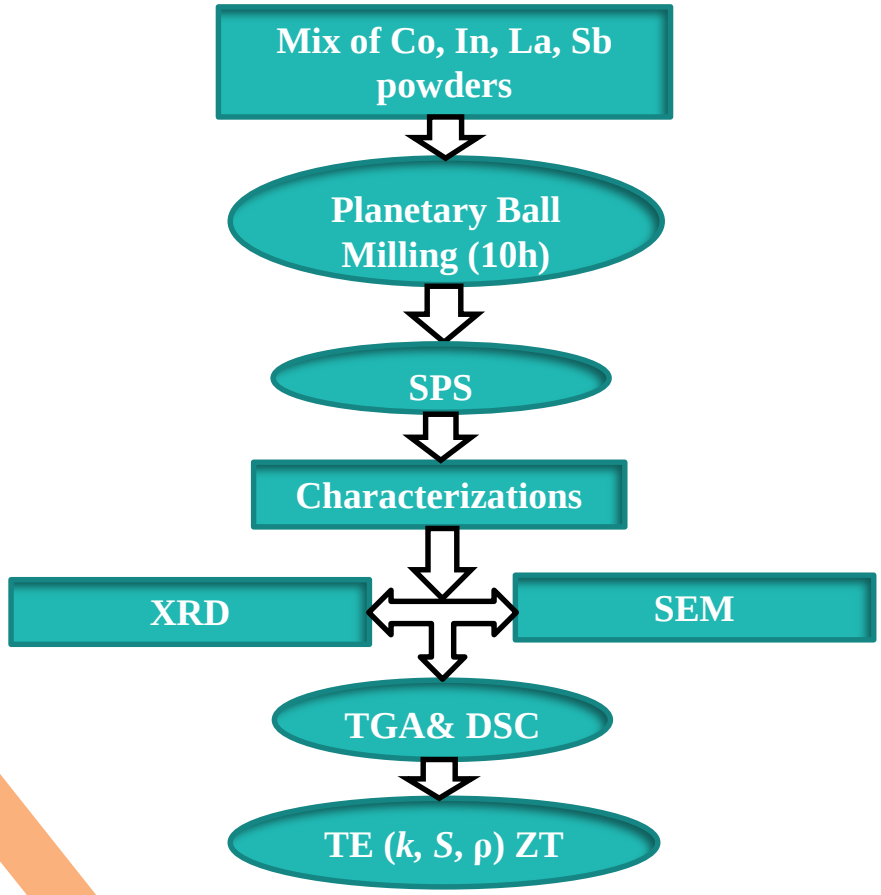


**Ball milling condition:**

- ✓Zirconia Jar 50 ml,
- ✓Zirconia balls 5 mm in diameter,
- ✓The weight ratio of balls to powders 20:1,
- ✓The speed 400 rpm,
- ✓Time 10 hrs.

**Spark plasma sintering (SPS) condition:**

- ✓Temperature 600°C,
- ✓Time for 10 min,
- ✓Pressure of 36MPa,
- ✓Cylindrical graphite die 10mm diameter,
- ✓Heating rate 100°C/min,
- ✓Vacuum atmosphere ~ 4 Pa.

# Methodology


Ball Milling

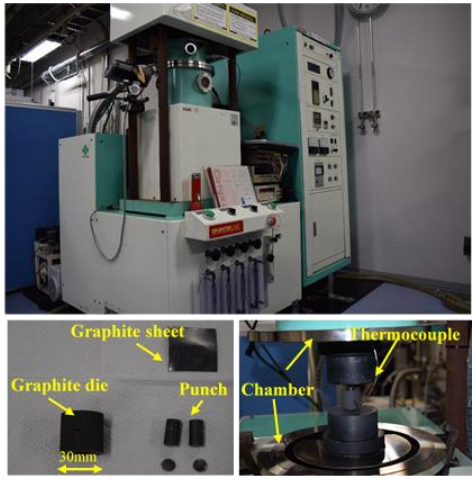


Spark plasma sintering (SPS)

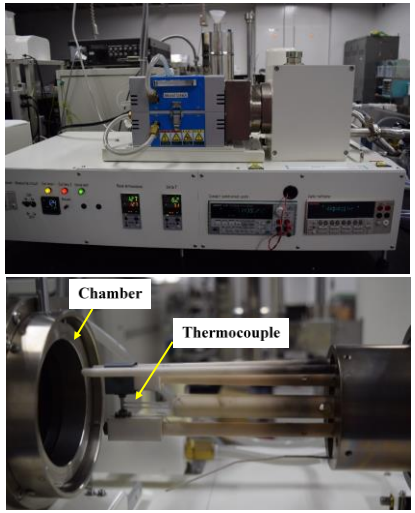


ZEM-3 system device

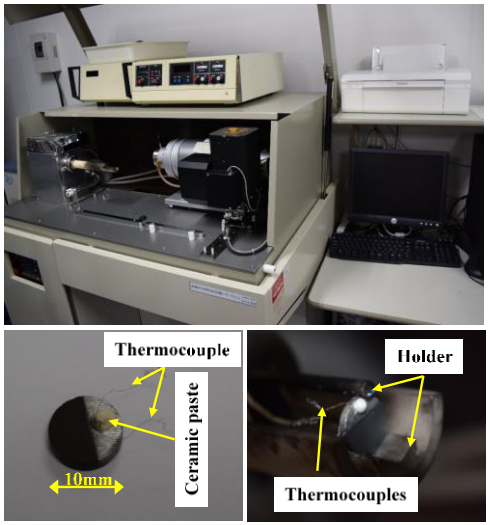


A laser flash system (TC-7000H)

Scanning Electron microscopy (SEM)

Simultaneous thermal analysis (STA)

# *Results and Discussion ... (Cont.)*

## In-added $La_{0.25}Co_4Sb_{12}$ compositions ($0 \leq x \leq 0.5$)

**Microstructure properties**

The dominated $CoSb_3$ structure of skutterudite phase

The space group of Im-3

InSb and $CoSb_2$ secondary phases.

InSb phase was observed in most filled samples except $In_{0.1}La_{0.25}Co_4Sb_{12}$ sample.

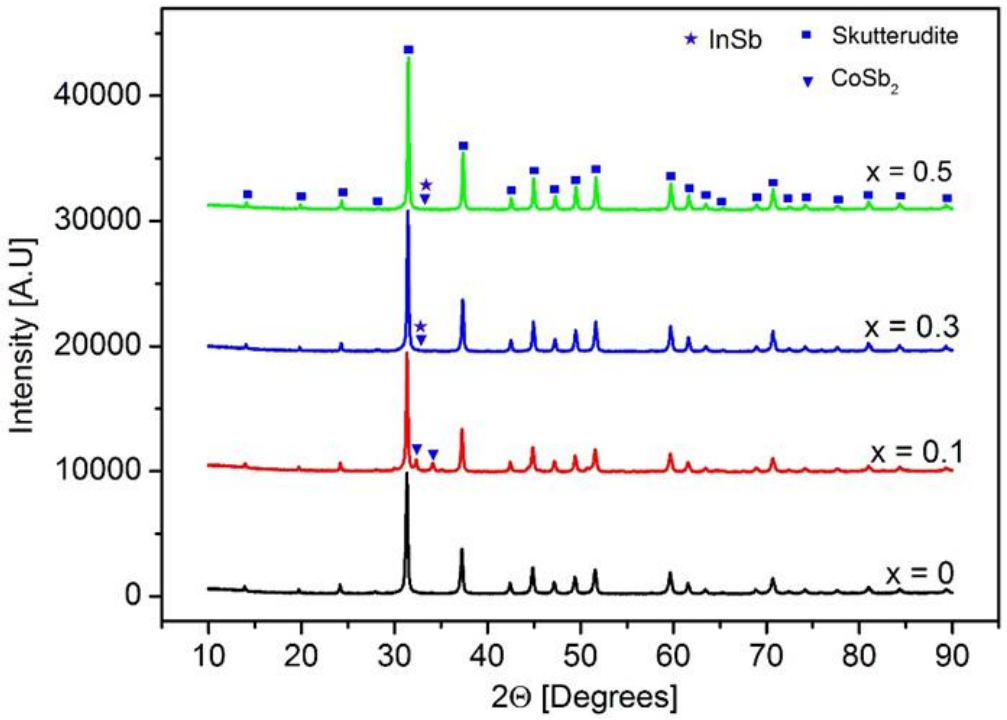

# *Results and Discussion … (Cont.)*

The main phase of skutterudite $CoSb_3$

Secondary phases including; $CoSb_2$ and $CoSb$.

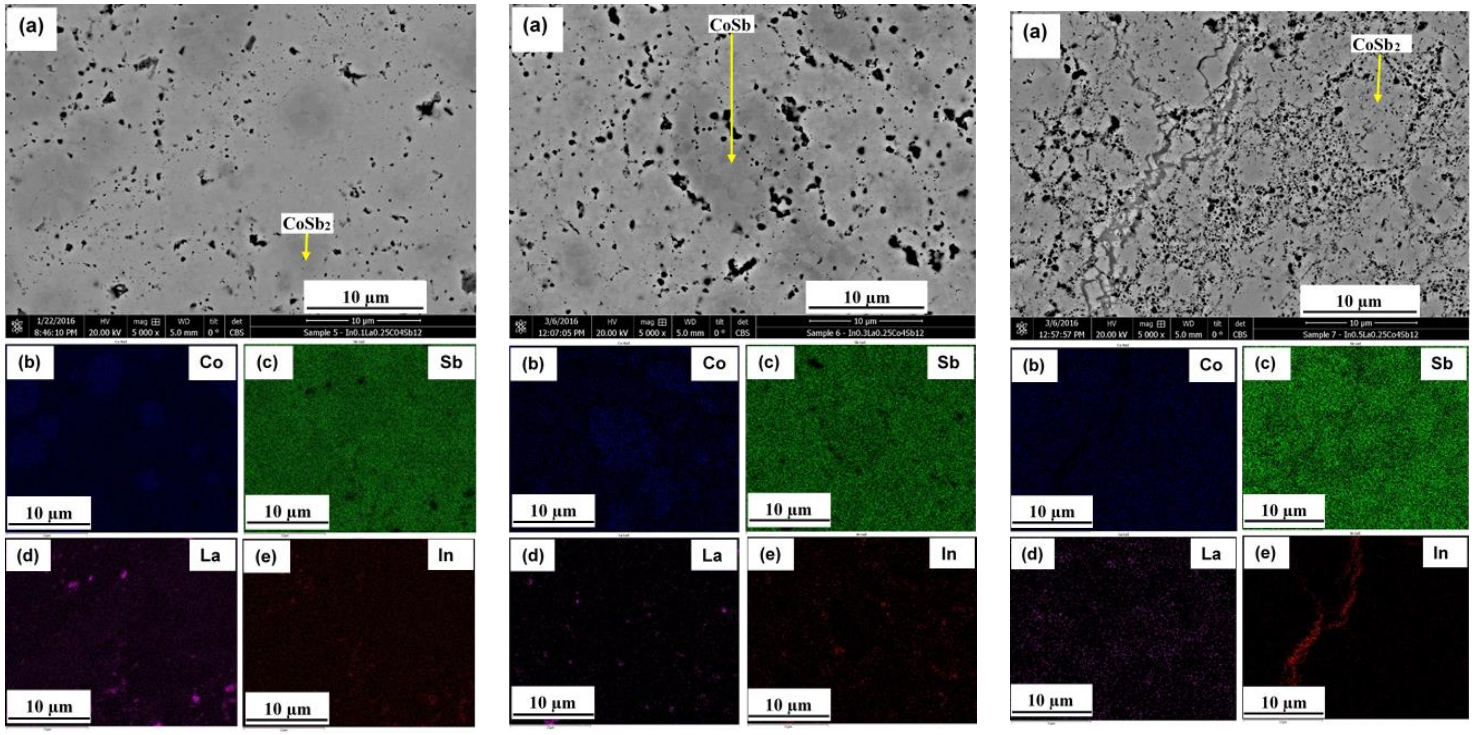


In=0.1 In=0.3 In=0.5

# Results and Discussion … (Cont.)

## In-filled $La_{0.25}Co_4Sb_{12}$ compositions ($0 \leq x \leq 0.5$)

**Microstructure properties**

- ✓ The dominated $CoSb_3$ structure of skutterudite phase
- ✓ The space group of Im-3
- ✓ InSb and $CoSb_2$ secondary phases.

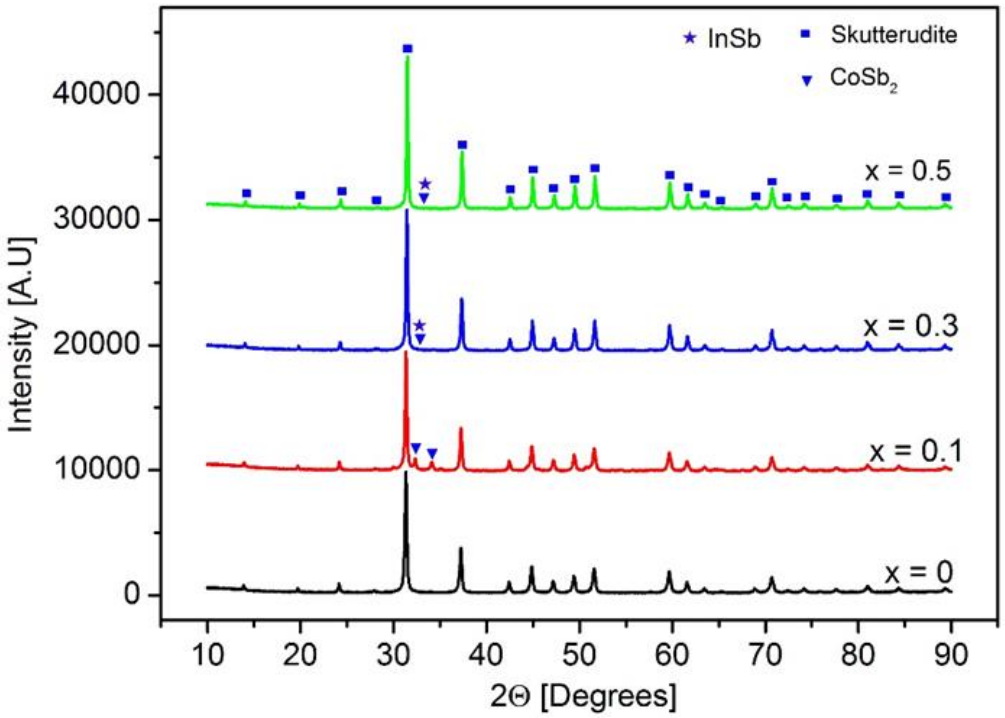

# Results and Discussion … (Cont.)

In was successfully filled the voids.

Atomic radius:

In (1.57 Å)

Void (1.892 Å)

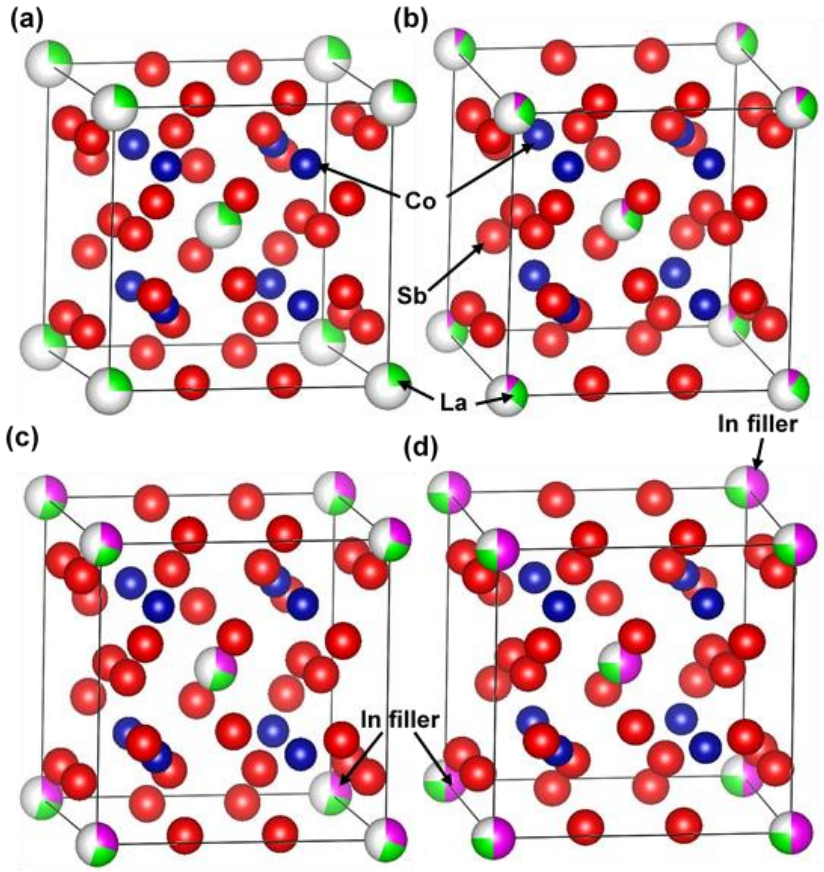


The Jana Refinement images of (a) In = 0, (b) In = 0.1, (c) In = 0.3 and (d) In = 0.5

# Results and Discussion … (Cont.)

**Thermoelectric Properties**

**Electrical resistivity**

The lowest electrical resistivity value obtained was **9.67 μΩm** which was achieved for In=0.5 sample at room temperature, this is mainly due to the presence of InSb phase and is relatively highly conductive as mentioned previously.

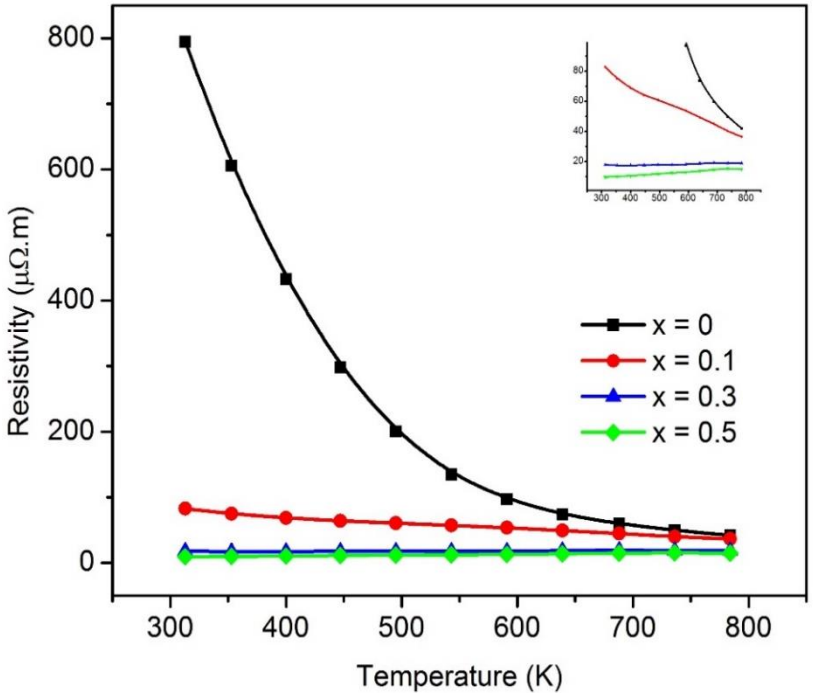

# Results and Discussion ... (Cont.)

S was changed from p-type to n-type
In atoms act as electron donors

The absolute **Seebeck** reached to a maximum value over measured samples of 252 μV/K at 495 K for x = 0.1 sample.

The **power factor** to the highest value of 3.85 x $10^{-3}$ W/m$K^2$ has been obtained for $In_{0.5}La_{0.25}Co_4Sb_{12}$ sample at 543 K

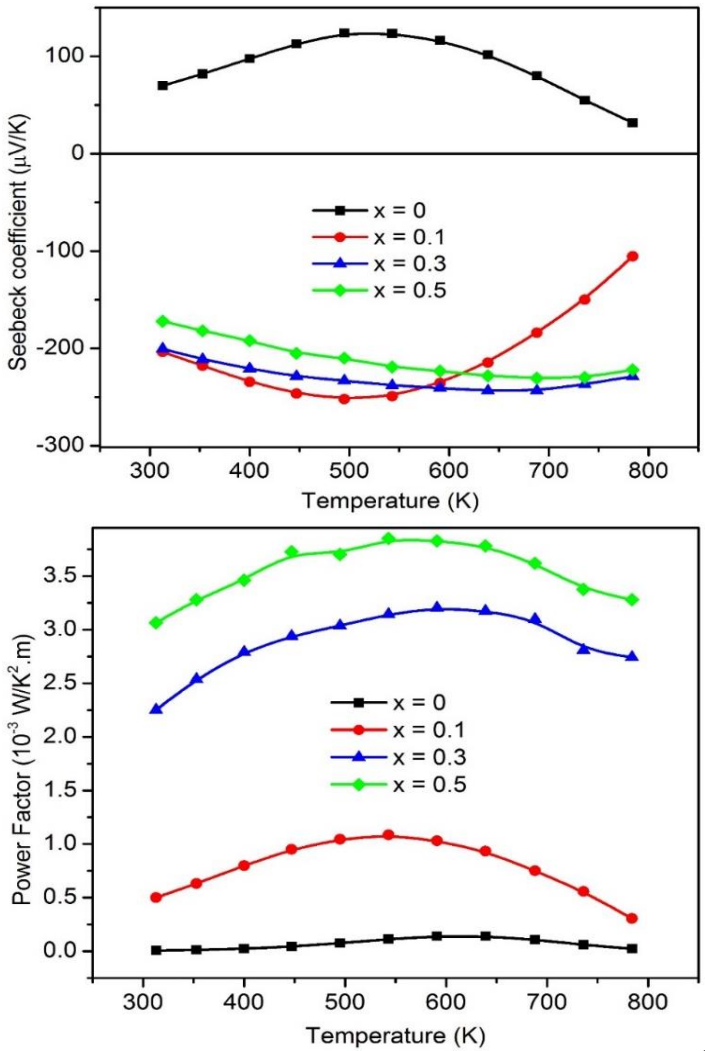

# Results and Discussion ... (Cont.)

The **thermal conductivity** was greatly minimized to 1.27 W/mK for $In_{0.1}La_{0.25}Co_4Sb_{12}$ sample at 495K.

The $In_{0.1}La_{0.25}Co_4Sb_{12}$ compound shows the lowest **lattice thermal conductivity** value of 1.14 W/mK which is obtained at 495K.

The average of electronic contribution $k_e$ is 18% from the total thermal conductivity.

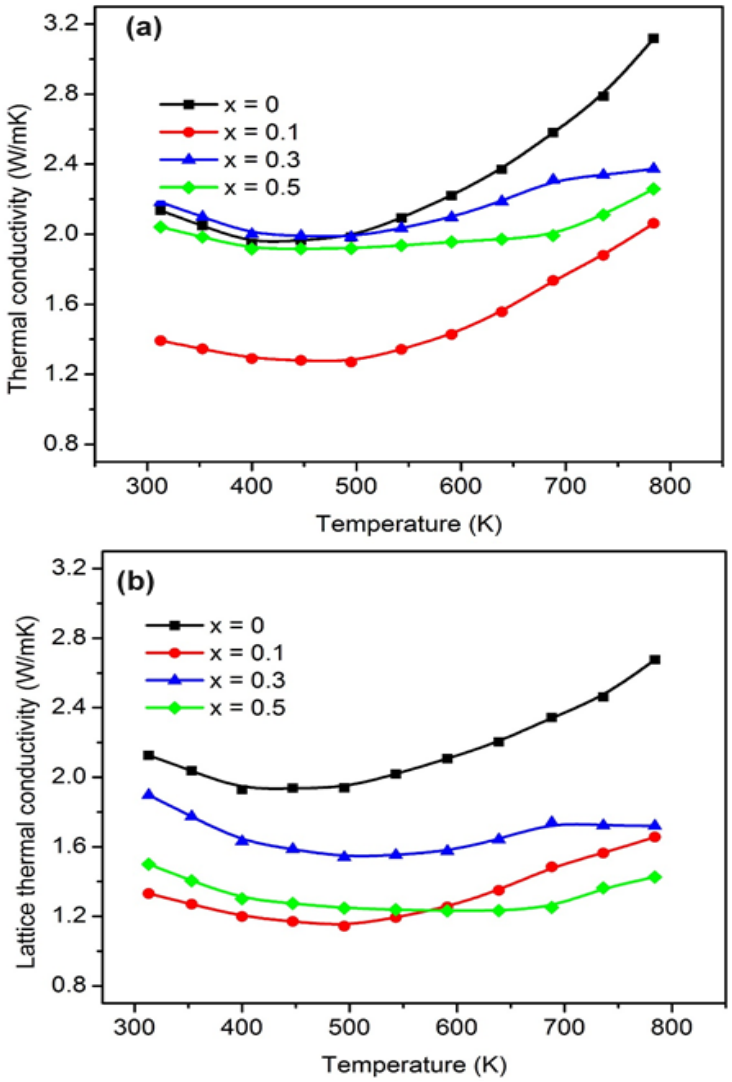

# Results and Discussion … (Cont.)

The maximum value of ZT was **1.25** observed at 688 K for $In_{0.5}La_{0.25}Co_4Sb_{12}$ sample, due to the substantial reduction in the lattice thermal conductivity.

The improvement is 8 % higher than $In_xLa_{0.5}Co_4Sb_{12}$ system

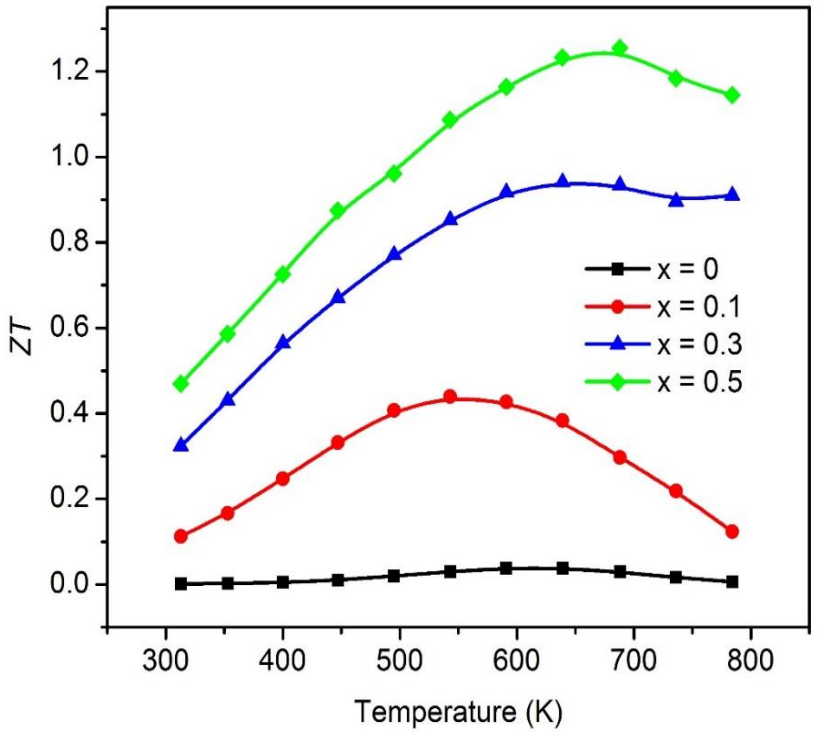

# Summary

| No | Compound | Exp. density ($g/cm^3$) | Th. density ($g/cm^3$) | $\rho_{min}$ (μΩm) | $S_{max}$ (μV/K) | $P.F_{max}$ ($10^{-3}$ × $W/K^2.m$) | $K_{tot,min}$ (W/mK) | $K_{Lmin}$ (W/mK) | $ZT_{max}$ |
|---|---|---|---|---|---|---|---|---|---|
| 1 | $La_{0.25}Co_4Sb_{12}$ | 7.53 | 7.78 | 42.1 @ 789 K | 124 @ 495 K | 0.14@ 591 K | 1.98 @ 495 K | 1.92 @ 400 K | 0.04 @ 591 K |
| 2 | $In_{0.1}La_{0.25}Co_4Sb_{12}$ | 7.43 | 7.82 | 36.5 @ 789 K | -252@ 495 K | 1.09 @ 543 K | 1.27 @ 495 K | 1.07 @ 495 K | 0.44 @ 543 K |
| 3 | $In_{0.3}La_{0.25}Co_4Sb_{12}$ | 7.66 | 7.89 | 17.5 @ 400 K | -243@ 688 K | 3.2 @ 591 K | 1.98 @ 495 K | 1.29 @ 543 K | 0.94 @ 639 K |
| 4 | $In_{0.5}La_{0.25}Co_4Sb_{12}$ | 7.88 | 7.99 | 9.7 @ 314 K | -231@ 688 K | 3.85 @ 543 K | 1.92 @ 495 K | 0.83 @ 639 K | 1.25 @ 789 K |

# Summary of results

| No. | Composition | $\rho_{min}$ (μΩ.m) | $\alpha_{max}$ (μV/K) | $PF$ ($10^{-3}$ W/m.K$^2$) | $K_{min}$ (W/m.K) | $K_{Lmin}$ (W/m.K) | $ZT$ | HV |
|---|---|---|---|---|---|---|---|---|
| 1 | Mn-added $CoSb_3$ | 33.2 @ 577 °C | 242 @ 127 °C | 0.39 @ 277 °C | 3.3 @ 500 K | 3.3 @ 500 K | 0.06 @ 600 K | 639 |
| 2 | Hf-added $CoSb_3$ | 52.1 @ 546 °C | 153 @ 153 °C | 0.14 @ 300 °C | 1.8 @ 400 K | 1.8 @ 400 K | 0.04 @ 500 K | 331 |
| 3 | $Al_{0.3}$-added $CoSb_3$ | 31.5 @ 527 °C | -251 @ 27 °C | 0.4 @377 °C | 4.6 @ 600 K | 4.4 @ 600 K | 0.05 @ 600 K | 499 |
| 4 | $Al_{0.6}$-added $CoSb_3$ | 38.4 @ 527 °C | 218 @ 127 °C | 0.4 @ 327 °C | 3.3 @ 500 K | 3.2 @ 500 K | 0.07 @ 600 K | 469 |
| 5 | $Al_2$-added $CoSb_3$ | 56.5 @ 527 °C | 218 @ 127 °C | 0.34 @ 277 °C | 2.7 @ 500 K | 2.6 @ 500 K | 0.06 @ 600 K | 436 |
| 6 | $Al_{0.1}$-added $Yb_{0.25}Co_4Sb_{12}$ | 5.5 @ 27 °C | -217 @ 577 °C | 4.9 @ 377 °C | 3.3 @ 300 K | 2 @ 400 K | 0.93 @ 800 K | 475 |
| 7 | $Al_{0.2}$-added $Yb_{0.25}Co_4Sb_{12}$ | 5.4 @ 27 °C | -208 @ 577 °C | 4.7 @ 327 °C | 3 @ 300 K | 1.3 @ 500 K | 0.87 @ 850 K | 456 |
| 8 | $Al_{0.3}$-added $Yb_{0.25}Co_4Sb_{12}$ | 7.6 @ 27 °C | -213 @ 577 °C | 4.3 @ 577 °C | 1.7 @ 300 K | 0.7 @ 500 K | 1.36 @ 850 K | 441 |
| 9 | $Bi_{0.1}$-added $Yb_{0.25}Co_4Sb_{12}$ | 30 @ 427 °C | 307 @ 77 °C | 1.3 @ 277 °C | 2.4 @ 850 K | 1.8 @ 850 K | 0.4 @ 850 K | 430 |
| 10 | $Al_{0.1}Bi_{0.05}$-added $Yb_{0.25}Co_4Sb_{12}$ | 22 @ 27 °C | -409 @ 277 °C | 5 @ 277 °C | 3.6 @ 600 K | 3.2 @ 600 K | 0.9 @ 600 K | 442 |


DOMINUS ILLUMINATIO MEA

# Themoelectrochemical Energy Harvesting

- Alternative to solid-state Thermoelectrics is **Liquid Thermoelectrics**.
- Liquid Thermoelectric cells are referred to as Thermo-electrochemical Cells. (**Thermocells** or **TECs**)
- Consitutents of Thermocells

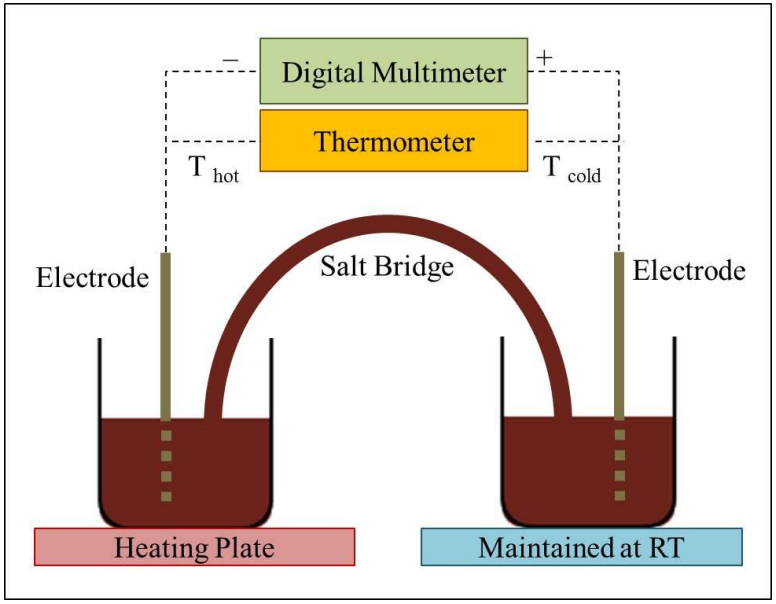


**Fig 2.** Two-beaker Thermocell

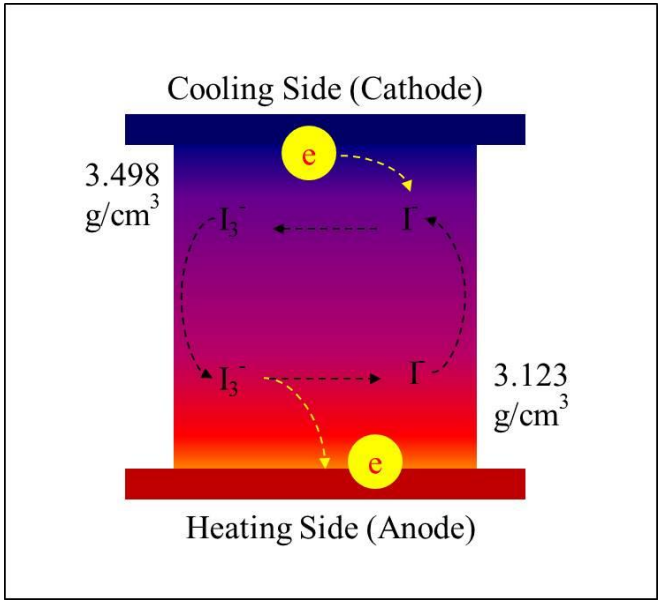


**Fig 3.** Cell Config. Thermocell

*REF: J. Electrochem. Soc (1995) 142, 11;*
*Nanoscale Microscale Thermophys. Eng. (2014) 17, 304*

# High Thermal Conductivity Reduces Power

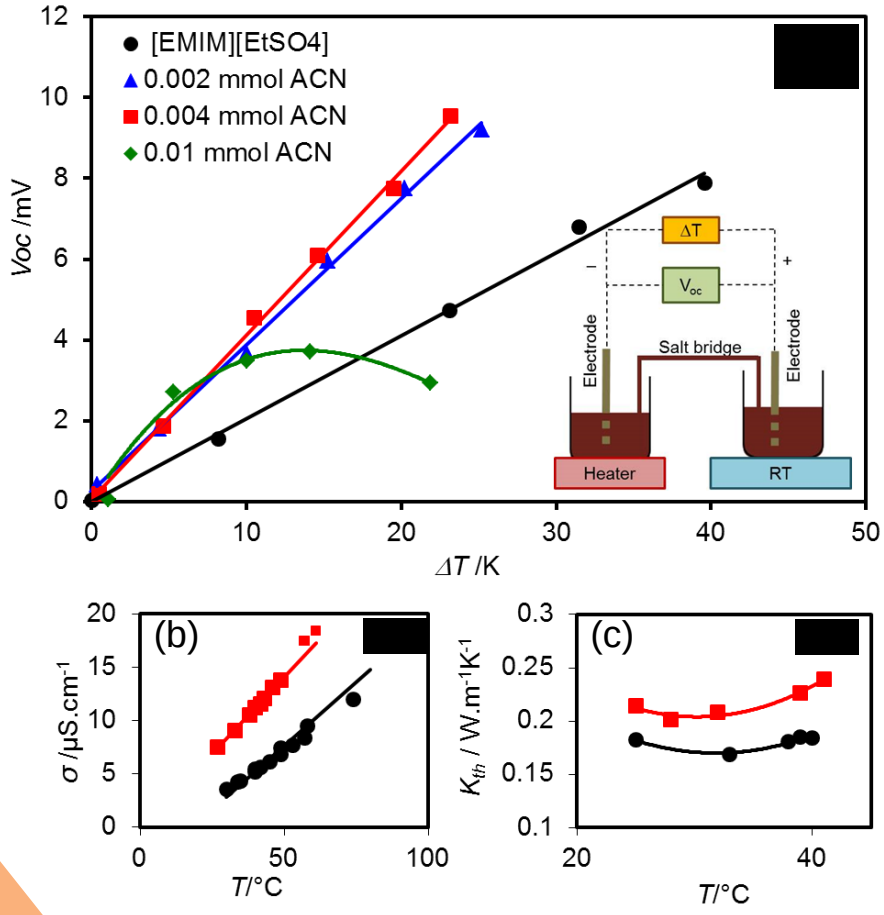


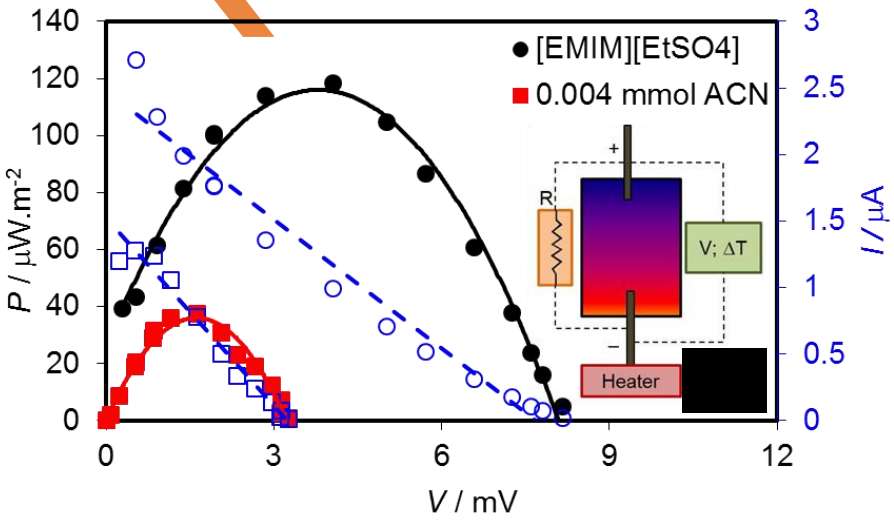








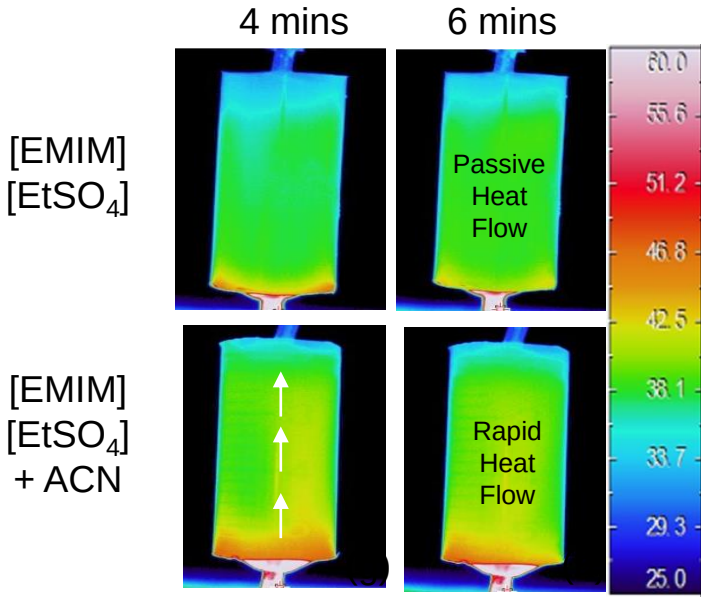


**Fig 5.** Polar solvent increases the ionic conductivity and Electrochemical Seebeck; however; it simultaneously increases the thermal conductivities. Therefore, reducing the output power density from **120 to 40 μW.cm$^{-2}$** .

*REF: SW Hasan et al, Sains Malaysiana (2018)*

# Experimental Details

**Electrolyte Preparation:** The $I^-/I_3^-$ redox solution (0.7 M) was prepared in 50 ml distilled water by dissolution of Iodine (5g) and Potassium Iodide (10g).

**PVDF Membrane Synthesis:** Commercially available Poly(Vinylidene Fluoride) (PVDF, Kynar® K-761, molecular weight of 440,000, density=1.7 g/ml and melt temperature ~ 165°C) powder was mixed with 1-Methyl-2-Pyrrolidinone (NMP) in a ratio of 18% by wt.

**Cell Fabrication:**

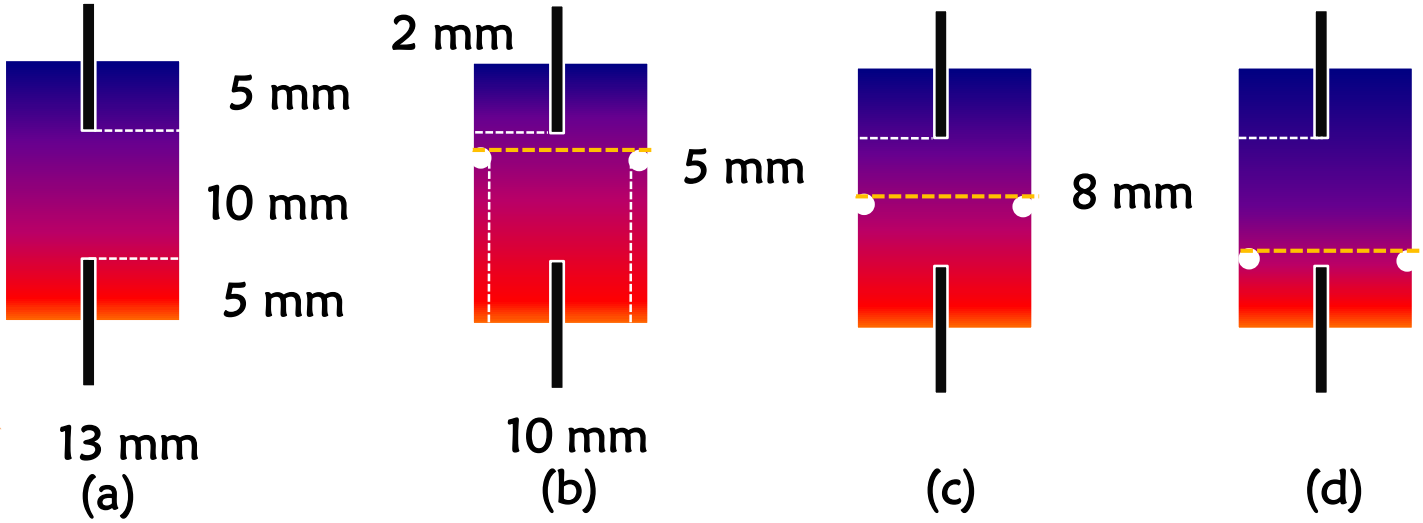




*SW Hasan et al, Sci. Rep. (2016), 6, 29328*

# Results & Discussion

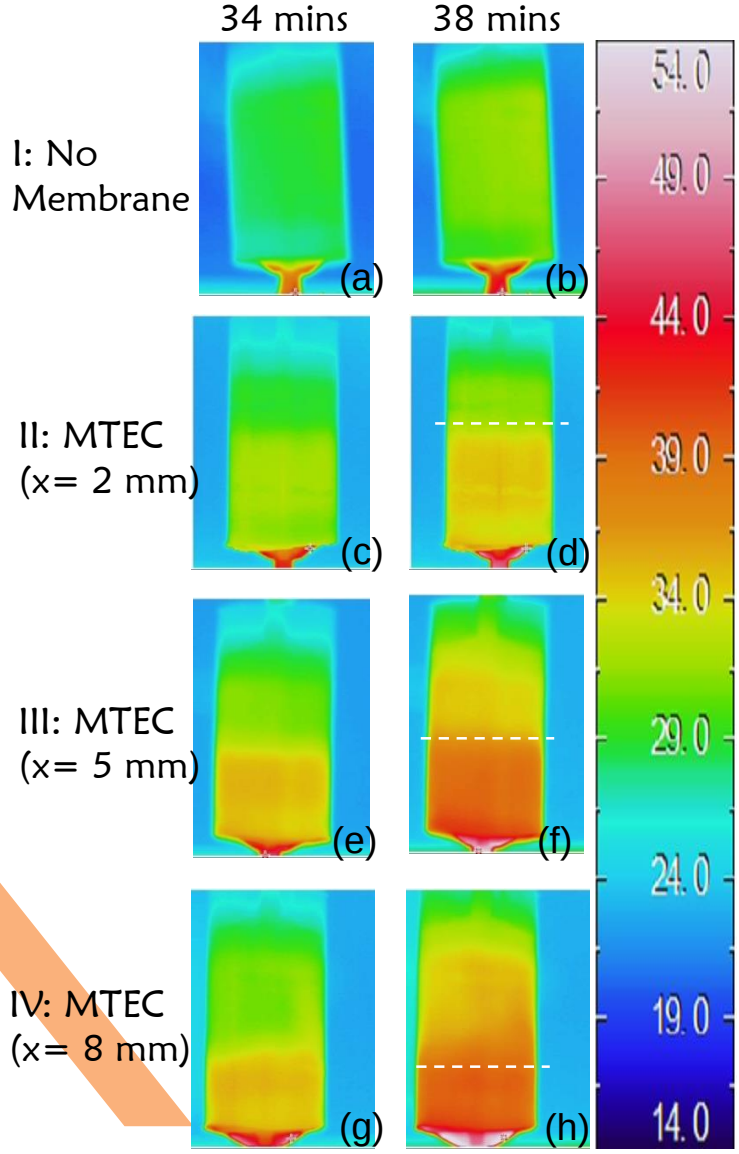


**Fig 7.** Infrared Thermography

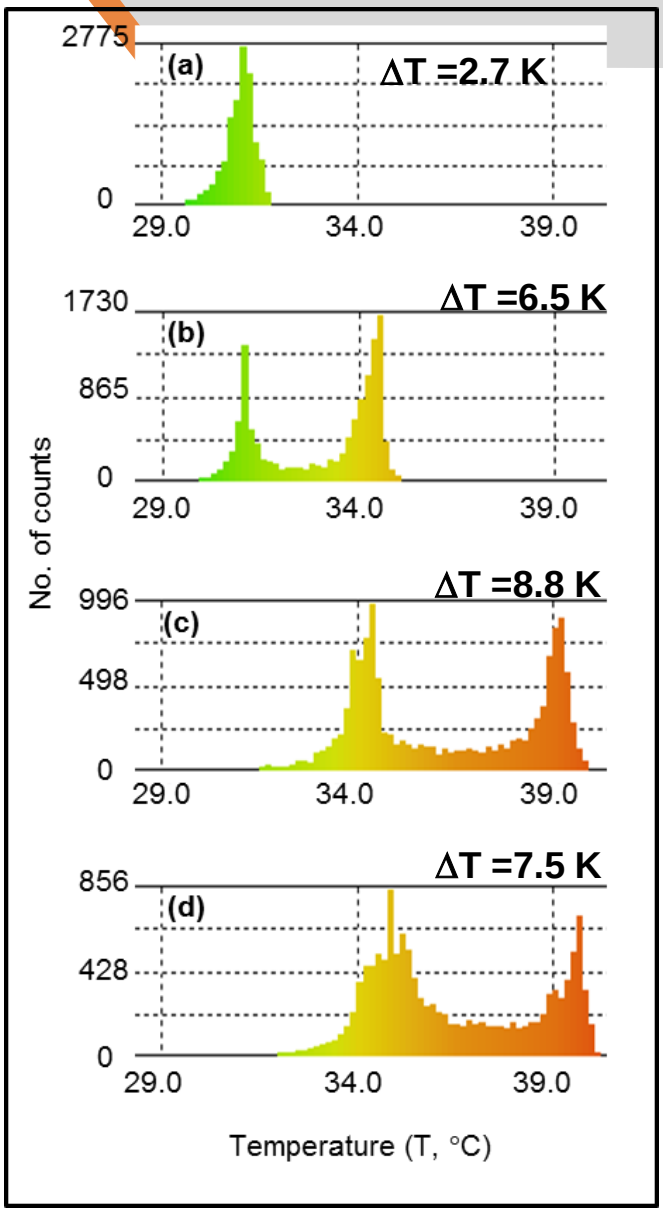


**Fig 8.** Thermal Histograms



*SW Hasan et al, Sci. Rep. (2016), 6, 29328*

# Conclusions

- The presence of the membrane is significantly useful to enhance the TEC performance.
- The open-circuit voltage of MTEC is almost **2 times** higher than the without membrane TEC.
- The maximum power density of the MTEC is **245 nWcm$^{-2}$** which is **78%** higher than the membrane-less case.
- The reason of this high performance is rooted in the thermal gradient improved by the PVDF membranes. The experiments show that the best MTEC (i.e. the membrane at the centre) simultaneously has highest thermal gradient of **8.8 K**.

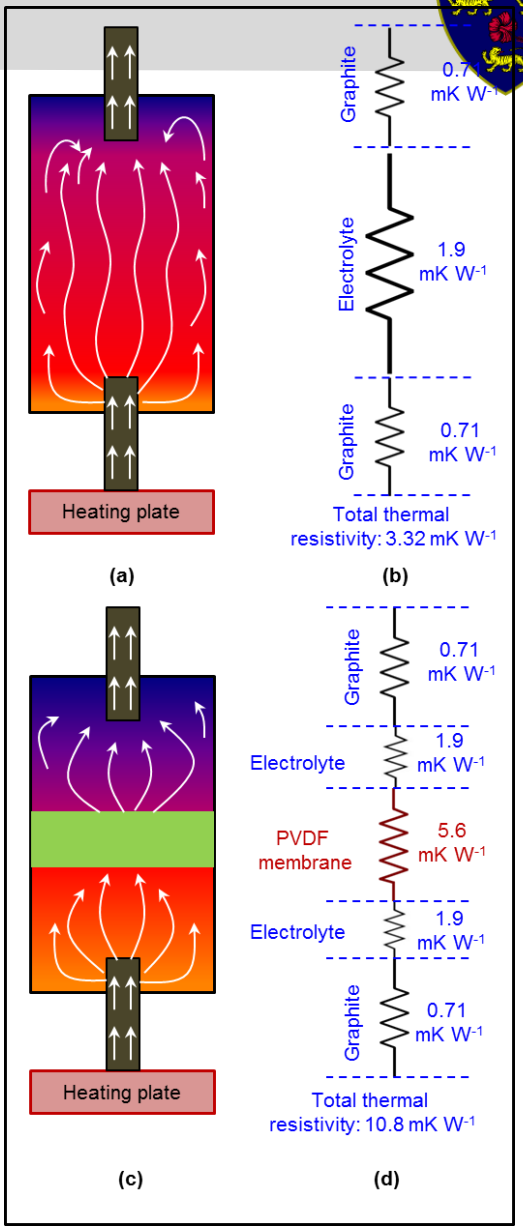


**Fig 9.** Thermal Resistive Model

# Strategies to Increase ZT

All approaches fall into one of three categories:

**1. Decrease the lattice thermal conductivity**

- Focus on phonons
- larger unit cell and higher mass to decrease sound velocity
- Increase disorder to decrease phonon mean free path

**2. Increase the carrier mobility**

- New, covalently bonded materials
- Heterostructures to physically separate carriers from scattering centers

**3. Increase the thermopower**

- Larger effective mass materials
- Barriers to inhibit transport of low energy carriers
- Novel band structures and/or scattering mechanisms

# Summary

The future of thermoelectricity relies on several important aspects:

1) One must find new mechanisms for balancing electron and phonon transport to maximize TE properties (high zT),
2) TE materials must be readily available and at low cost, and their processing must be simple and rapid to suit large-scale industrial operation,
3) It is important to focus on the design of high-performance TE materials that meet the actual application demands, especially to possess high average values of zT and have their performance peaking in the desired regime of operation temperatures,
4) It is imperative that the modules are thermally and mechanically stable and have a long lifetime,
5) It is important to specify proper and efficient synthesis routes and module fabrication processes to make thermoelectricity economically viable.


# THANK YOU

Office of the Deputy Vice-Chancellor
(Academic & International)
Level 9, Chancellery
University of Malaya
50603 Kuala Lumpur, MALAYSIA.
Tel: +603-79673203 | Fax: +603-79572314
Website: www.um.edu.my